ESTIMATION OF DUST AND SAND INDUCED IMPAIRMENTS ON SATELLITE LINKS

BY

Muhammad Omair Butt

A Thesis Presented to the
DEANSHIP OF GRADUATE STUDIES

KING FAHD UNIVERSITY OF PETROLEUM & MINERALS

DHAHRAN, SAUDI ARABIA

In Partial Fulfillment of the
Requirements for the Degree of

MASTER OF SCIENCE

In

ELECTRICAL ENGINEERING

APRIL 2014

KING FAHD UNIVERSITY OF PETROLEUM & MINERALS

DHAHRAN- 31261, SAUDI ARABIA

DEANSHIP OF GRADUATE STUDIES

This thesis, written by **Muhammad Omair Butt** under the direction his thesis advisor and approved by his thesis committee, has been presented and accepted by the Dean of Graduate Studies, in partial fulfillment of the requirements for the degree of **MASTER OF SCIENCE IN ELECTRICAL ENGINEERING.**

Dr. Kamal M. Harb
(Advisor)

Dr. Ali Ahmad Al-Shaikhi
Department Chairman

Dr. Samir H. Abdul-Jauwad
(Co-Advisor)

Dr. Salam A. Zummo
Dean of Graduate Studies

Azzedine Zerguine

Dr. Azzedine Zerguine
(Member)

9/6/14
Date

Shaikh Sharif

Dr. Sheikh Sharif Iqbal
(Member)

K. Qureshi

Dr. Khurram Karim Qureshi
(Member)

Dedication

To my Parents, brother and sisters, for their endless love and support

ACKNOWLEDGMENTS

I express my deep gratitude to my advisor Dr. Kamal M. Harb and co-advisor Dr. Samir H. Abdul Jauwad for their supervision, guidance, assistance and valuable comments throughout the progress of my research.

I would like to thank my thesis committee members Dr. Azzedine Zerguine, Dr. Sheikh Sharif Iqbal and Dr. Khurram Karim Qureshi for their guidance.

I am thankful to my friends for their support and joyful company during the course of my MS program at KFUPM. I am also thankful to King Fahd University of Petroleum & Minerals (KFUPM) for supporting this thesis.

Last but definitely not the least, my warmest acknowledgments to my parents and siblings for graciously extending their support and encouragement to me during my time at KFUPM and for many years prior to that.

TABLE OF CONTENTS

LIST OF TABLES

LIST OF FIGURES

LIST OF ABBREVIATIONS

UL : Up Link

DL : Down Link

ISPs : Internet Service Providers

VHF : Very High Frequencies

TEC : Total Electron Content

SNR : Signal to Noise Ratio

EDS : Enhanced Decision System

NOGAPS : Navy Operational Global Atmospheric Prediction System

EMW : Electromagnetic Wave

QoS : Quality of Service

DSS : Decision Support System

CECCR : Center of Excellence for Climate Change Research

ES : Earth Station

Tx : Transmit

Rx : Receive

THESIS ABSTRACT

Name: Muhammad Omair Butt

Title: Estimation of Dust and Sand Storms Induced Impairments on Satellite Links

Major Field: Electrical Engineering

Date of Degree: April, 2014.

Dust and sand storms are a significant cause of wireless channel impairments, often observed in arid and semi-arid areas of the world. Measurement of such weather induced impairments is an essential component for evaluating optimal link budgets of satellite communication links. Thus, utilization of superfluous radio resources can be avoided or at least minimized by precise impairment estimations while guaranteeing reasonable quality of service. Furthermore, dust and sand storms can be regarded as a complex meteorological phenomenon because the dust characteristics vary greatly for different locations. Study of regional surface characteristics gives necessary information about probable intensity and altitudes of dust storms arising in that area. The altitude based non-uniformity of dust and sand concentration in individual storms also needs to be taken into consideration. Several parameters including visibility, average dust particles size, permittivity indices, just to name a few, are required for quantifying the weather impairments and acquiring estimates. This study encompasses development of a modified

physical model for dust storms having several visibility dependent horizontal layers with reference to variations in altitude along with probabilistic dust and sand particle sizes distribution in each layer. As evident from simulation results in the presence of proposed enhance system, such strategies would help in obtaining accurate impairment estimates, assisting to optimally design the link budgets.

ملخص الرسالة

الاسم الكامل: محمد عمير بوت

عنوان الرسالة: مدى تأُثير العواصف الترابية والرملية على الاتصالات عبر الأقمار الإصطناعية

التخصص: هندسة كهربائية

تاريخ الدرجة العلمية: نيسان 2014

تعتبر العواصف الترابية والرملية هي من أحد الأسباب المؤثرة في الإتصالات اللاسلكية، والتي توجد عادةً في المناطق الصحراوية وشبه الصحراوية في العالم. فإن قياس مثل هذه التأثيرات التي يسببها الطقس يعتبر عنصراً أساسياً لتقييم الميزانيات الأمثل للاتصالات عبر الأقمار الإصطناعية. وبالتالي، فإن استخدام موجات الراديو الزائدة عن الحاجة يمكن تجنبها أو على الأقل التقليل منها من خلال تقديرات دقيقة لنسبة تأثير تقلبات الطقس مع ضمان خدمة ذات جودة معقولة. وعلاوة على ذلك، يمكن اعتبار الغبار والعواصف الرملية من أحد ظواهرالأرصاد الجوية المعقدة لأن خصائصها تختلف اختلافا كبيرا من موقع إلى أخر. فدراسة خصائص منطقة الإرسال يعطي المعلومات الضرورية حول كثافة وارتفاعات من العواصف الترابية المحتملة التي تنشأ في هذا المجال. أيضاً إن عدم صحية تمثيل إنتشار الغبار والرمال في العواصف على أساس الارتفاع بحاجة لأن تؤخذ بعين الاعتبار. من هنا فان العديد من المعطيات الضرورية مثل الرؤية، على سبيل المثال لا الحصر، ومتوسط حجم جزيئات الغبار، والمؤشرات السماحية تستخدم لقياس تقلبات الطقس والحصول على تقديرات تقريبية مماثلة للواقع. وعليه فان هذه الدراسة تشمل تطوير نموذج تمثيل صحيح للعواصف الترابية على شكل طبقات أفقية متعددة تعتمد الرؤية مع الإشارة إلى

الاختلافات في الارتفاع مع احتمالية توزيع جسيمات الغبار والرمال ذات الأحجام المختلفة في كل طبقة. كما يتضح من النتائج الموضحة في هذه الاطروحة استحداث نظام ذكي، وذلك فإن مثل هذه الاستراتيجيات تساعد في الحصول على تقديرات دقيقة لقيمة تاثيرات التقلبات المناخية، والتي تساعد في تصميم أمثل لميزانية الارتباط عبر الأقمار الاصطناعية.

CHAPTER 1

INTRODUCTION

Transformation of our world into a global village has only been possible due to extreme advancement in wireless communication technology. Optimum utilization of wireless medium is one of the most sought for areas in communications. Attenuation is observed to increase sharply with the increase in transmission frequencies. Therefore, it becomes difficult to optimally manage the shared resources in satellite dependent networks during weather impacted conditions. To improve the Quality of Service (QoS), an effective solution with the ability of better prediction, estimation and identification of all the involved attenuation factors is required.

1.1 Satellite Communication

Satellite communication technology is being used for provisioning of telecommunication services including interactive voice, multimedia and data services. It has a global impact on the communications, on contrary to the corresponding terrestrial communication links, as its link cost is independent of distance. Satellite communication systems are based on two key components: a ground segment and a space segment. A fixed or mobile entity along with the supplementary equipment is considered to be the ground segment. Similarly, the satellite stations being launched in space are regarded as the space segment. Satellites are usually regarded as regenerative repeater points, receiving the microwave radio signals, amplify them and retransmit to other points. Several of the reception devices on ground include satellite telephones, mobile reception equipment in aircraft and direct-to-home satellite equipment.

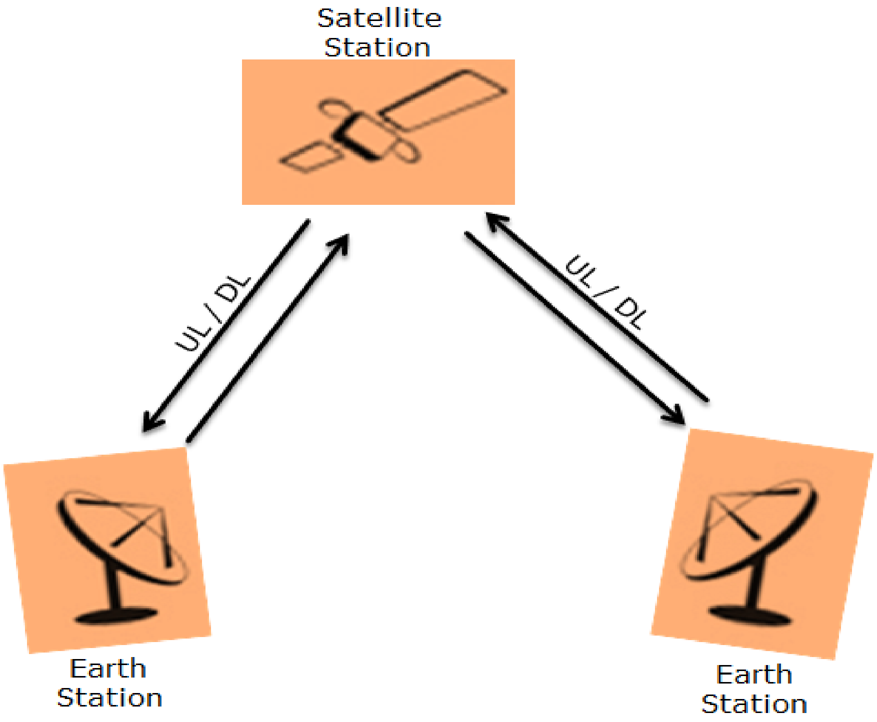

Figure 1.1: Satellite Communication System

Fig. 1.1 depicts a basic satellite network topology including ground stations interlinked via the satellite station. Furthermore, the uplink (UL) and downlink (DL) frequencies are assigned according to a proper frequency allocation plan, in accordance to the offered services. Such networks face radio channel impairments during weather deteriorated conditions including dust and sand storms [1]–[6], rainfall and other weather anomalies.

1.1.1 Applications of Satellite Technology

Tremendous advancements in the telecommunication technology have given rise to a healthy satellite services sector. Satellite communication networks provide services to broadcasters, Internet service providers (ISPs), governments, the military. The provided services can be divided into three distinct categories i.e. telecommunications, broadcasting and data communications.

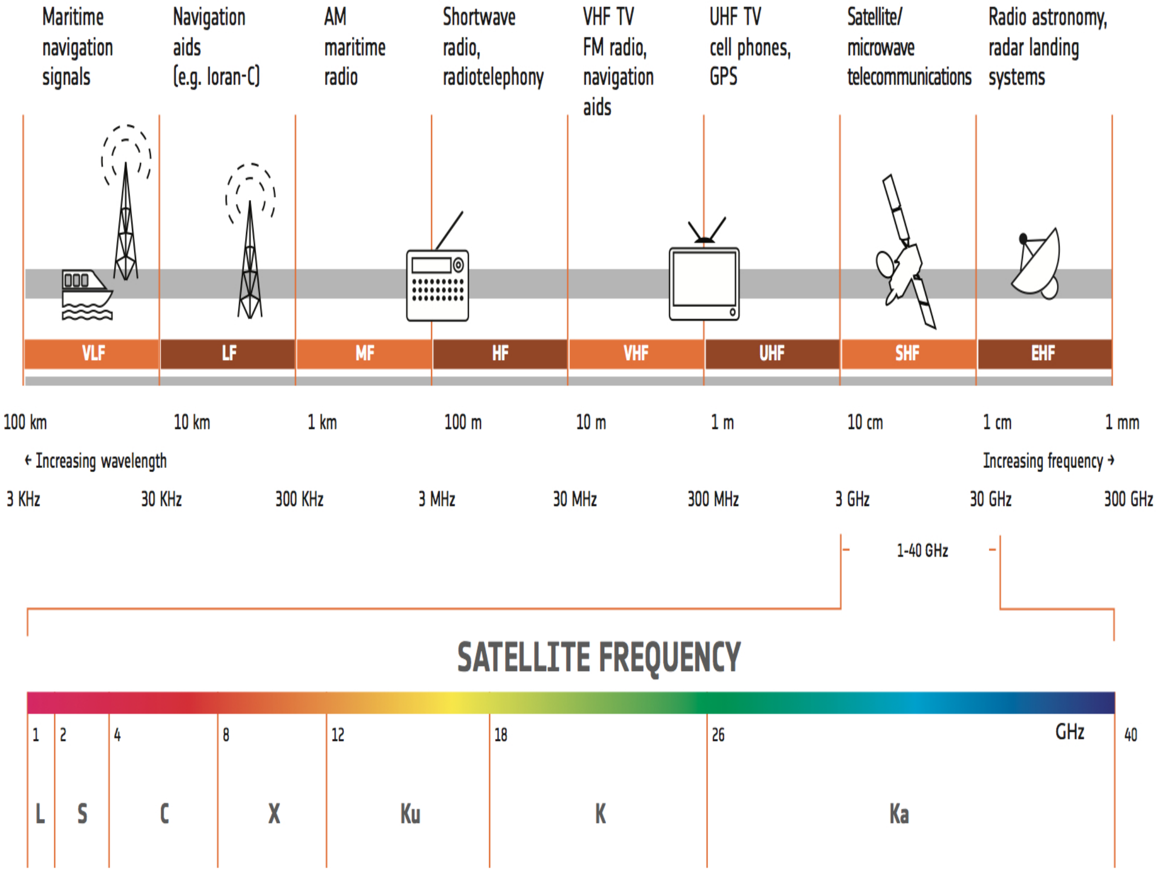

Figure 1.2: Frequency Bands [7]

Several designations have been made, in order to refer to the frequency bands being used for satellite communications, as depicted in Fig. 1.2. Operating at high frequency bands give leverage of having a wider bandwidth. On the other hand, the higher frequencies are more prone to signal degradations due to anomalous weathers such as dust and sand storms [1]–[6], atmospheric absorption and rainfall. With the passage of time, a considerable increase in the applications offered by satellite technology has been observed. Now a day, the intelligent satellite terminals are also used for astronomy, weather forecasting and mapping. Due to the substantial increase in the use satellite communication technology, congestion has become a critical issue. Several techniques on incorporating the higher order frequency bands are also being researched to increase the channel bandwidth.

1.2 Ionospheric Impairments

Usually, the radio wave frequencies higher than 100 MHz can easily pass through the ionosphere. But sometimes due to the presence of free electrons and the earth's magnetic field, the characteristics of such radio wave signals may be altered. The impairments induced due to bulk ionization include absorption, propagation time delay, polarization rotation and refraction.

The aforementioned impairing features vary with the position on earth and with time according to various long and short period changes of the ionosphere. The existence of small scale regularities in the electron concentration also causes relatively rapid fluctuations of a number of signal parameters, these fluctuations are collectively referred to as scintillation. Fig. 1.3 presents the phenomenon of scintillations.

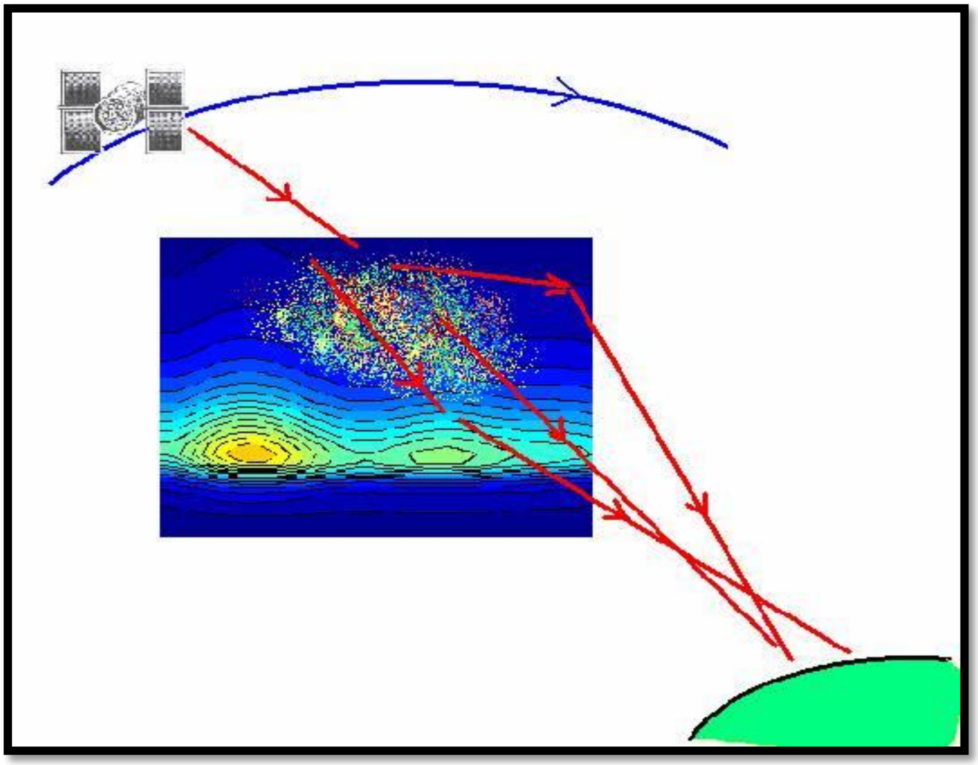

Figure 1.3: Ionospheric Scintillations – Absorption, Diffraction and Scattering [8]

1.2.1 Ionospheric Scintillation

Scintillations causing signal fluctuations in terms of amplitude, phase, polarization and direction of arrival may represent practical limitations to space communication systems. Scintillations are commonly observed at very high frequencies (VHF) and may occur at frequencies at least up to $7\,GHz$. Scintillation activity is mostly a night-time phenomenon. It is severe in the vicinity of geomagnetic equator and at high altitudes, least severe at mid-altitudes and increases with solar and geomagnetic activity.

1.2.2 Ionospheric Absorption

The absorption for a one-way traversal of radio wave at middle latitudes on normal incidence is generally less than 0.1 dB for frequencies greater than 100 MHz. Whereas, due to enhanced Ionospheric absorptions resulting from the solar flares and during auroral and polar-cap events, an upper limit of about 5 dB absorption on the radio wave should be expected.

1.2.3 Ionospheric Effects depending upon Total Electron Content (TEC)

It is significant in the determination of phase path, group delay, dispersion, refraction and Faraday polarization rotation of transionospheric radio signals. Usually, TEC is represented as the integral of electron concentration along the ray path. All the impairing constituents induced are directly proportional to the TEC.

1.3 Tropospheric Impairments

In addition to the thermal-noise radiations from any absorbing constituent in troposphere, the following factors need to be considered:

- Dust and sand storms impairments
- Clouds and precipitation impairments
- Atmospheric or gaseous absorption
- Various aspects of refraction and depolarization by precipitation

In general, the weather impairment effects become increasingly important for frequencies higher than $3\,GHz$. Surprisingly, significant attenuation can occur even in clear conditions for the radio waves above $40\,GHz$ in the region of absorption lines of water vapor and oxygen.

1.3.1 Dust and Sand Storms Impairments

Electromagnetic wave propagation in dust and sand storms has received some attention in the literature owing to its impairing impacts on the satellite communication technology, remote sensing and radio relay. This weather anomalous impairment constituent is observed in arid and semi-arid regions of the world. In this scenario, the radio wave passes through a dust and sand filled patch of air. Fig. 1.4 shows a dust and sand storm in effect at Dhahran, Saudi Arabia during April 2013.

Figure 1.4: Dust and Sand Storm, Dhahran [5]

A number of investigators have presented models to compute microwave attenuation in dust storms and concluded that attenuation by dust storms is not serious except for very dense storms [1]–[6]. However, dust and sand storms are complex to model and difficult to be measured accurately. The key parameters to mathematically model dust and sand storms include visibility, dust and sand particles sizes.

1.3.2 Gaseous/Atmospheric Absorption

While traversing through atmosphere, the radio waves experience phenomenon of energy absorption due to presence of several gases. A method for predicting such absorptions has been presented in [13]. The mathematical model for impairment computations involves parameters such as frequency, path elevation angle, height above mean sea level and the water vapor density. The percentage of water vapors in atmosphere is responsible for variations in gaseous absorption. Water vapor density usually follows normal probability law [14]. The average annual water vapor density can be used in order to present the approximate gaseous absorption for a certain region.

1.3.3 Precipitation/Rain and Clouds Impairments

The modelling of impairments induced by rain have been sought out by several research groups and is considered to be among the significant causes of satellite channel impairments. Rainfall impairment estimation models can be subdivided into the following two categories,

- Strategies related to defining physics of the process and modelling the constituents.
- Empirically finding the estimations with simplified assumptions

Pertaining to unavailability of many physical inputs needed to provide accurate results, the empirical estimation approaches are often used while assuring the precision of impairment estimates to a certain acceptable level. The Working Party 3M has analyzed all the leading rain attenuation models [15] and has given highest rank to the empirical models with better formulation, one of those models is the current procedure of ITU-R [13]. Fig. 1.5 presents the physical description of a rainfall event along with the clouds formation effecting the radio wave for satellite communication.

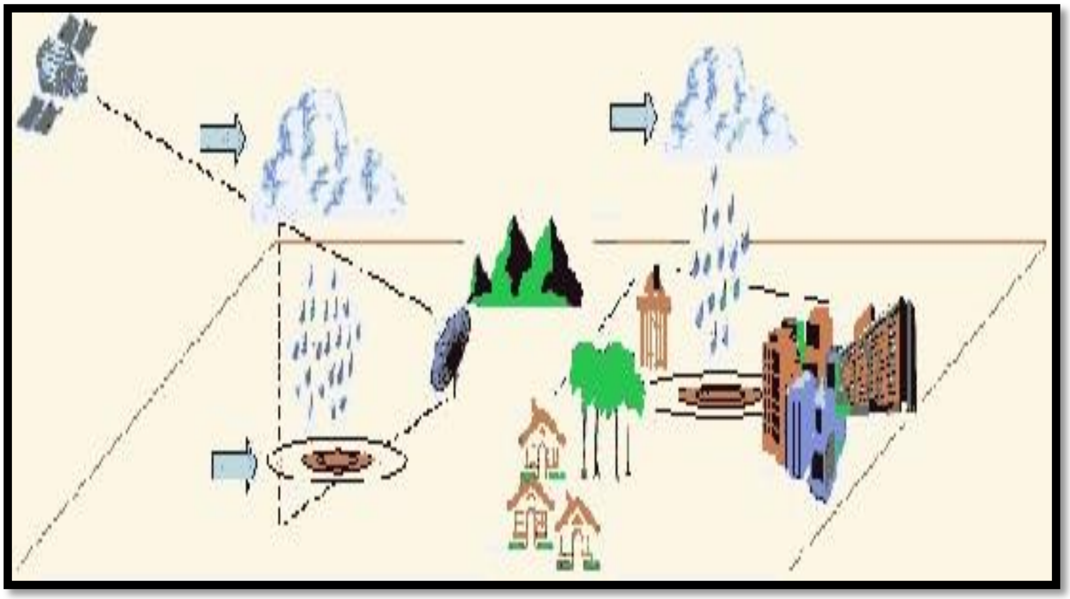

Figure 1.5: Clouds and Rainfall [9]

Similarly, several strategies have been devised for the estimation of impairments induced due to clouds [16]–[18]. The evaluations for these models have shown that either the formulation for a general purpose application is difficult or they lead to poor impairment estimations. An assessment of several models for cloud attenuation have been presented in [19]. To comprehensively incorporate the cloud impairments into a prediction procedure, a clear demarcation of the end points should be done for the cumulative distribution of path attenuation. The clear-sky condition can be considered as an end point with minimum attenuation, whereas a point with in the path having light rainfall can be considered as the maximum attenuation end point.

1.4 Other Impairing Factors

1.4.1 Low-Angle Fading

During the still air conditions, atmosphere usually tends to form layers with decreasing refractive index. Such variations have no effect on elevation angles well above 10^o for the satellite links. Whereas, the radio signals to and from satellite may be at grazing incidence to the tilted air and air refractive index boundary for the links with elevation angles below 10^o. The variations in position of the boundary of refractive index according to the signal path can induce large variations in energy levels at the ends of the signal path due to the relative movement of atmospheric layers and radio wave path. Large scale refractive irregularities across the layer boundary are responsible for such energy level variations and have a minimal dependence on radio frequency, in contrast to tropospheric scintillation, induced due to small scale refractive index changes with strong frequency dependence [13].

1.4.2 Melting Layer Attenuation

The region around $0^o\ C$ isotherm is regarded as melting layer. Rain drops are formed due to the ice and snow particles present in this region. It thickness D_m is approximately of the order of 500 m. Similarly, a distinct layer also referred to as radar bright band exists only for relatively low rain rates [20]. Low elevation links are more susceptible to experience significant impairments due to melting ice particles. Furthermore, these impairments are usually lesser than the rainfall impairments underneath. Several approaches to model this impairment have been discussed in [21], [22].

1.5 Thesis Outline

In Chapter 1, a brief overview of the satellite communication systems, their applications and the available frequency bands for communications is presented. Afterwards, several weather based impairment factors influencing the satellite communications have been described and finally the key objectives of thesis work have been mentioned.

Chapter 2 discusses the literature reviews of the factors influencing dust and sand storms and their effects on satellite communication links. Several research studies related to the empirical and experimental approaches for evaluating such weather anomalous impairments are presented. Finally, the work done in order to design an enhanced decision system (EDS) for signal to noise ratio (SNR) improvement has been presented.

Chapter 3 discusses the experimental analysis for several dust and sand samples taken from the Eastern province of Saudi Arabia. Based on the uncorrelated characteristics and behavior of dust and sand storms, the forecasted weather reports related to several environmental parameters are also illustrated for a few days in Saudi Arabia. Finally, the Sieve and Hydrometer analysis results of dust and sand samples are presented.

Chapter 4 presents the modified methodology used to develop a mathematical basis for impairment estimations. The idea of visibility increase in vertical direction has been elaborated along with the dust and sand particles size as well as concentration variation. The concept of layering the dust and sand storms in accordance to the visibility increase is explained. Furthermore, simulations related to the point and dust attenuation have been presented for several probable cases of dust and sand distributions namely, the uniform and normal. Lastly the impairment estimations have been done by incorporating the samples analysis details gathered in Saudi Arabia region.

In Chapter 5, an EDS has been designed. This EDS has the capability to immunize the satellite signal to some extent in lieu of weather impairments, specifically the dust and sand attenuations. The algorithmic basis for SNR calculations have been explained. Furthermore, the simulations before and after incorporating the EDS have been presented.

Chapter 6 includes a brief summary of the work, conclusions and future recommendations.

1.6 Thesis Objectives

The key aim of this research is to devise an effective strategy for dust and sand storms induced attenuations on microwave links. Following are the major issues that will be considered in this thesis:

1. A comprehensive literature review of currently available models for quantifying the dust and sand storms effects on satellite communication links.
2. Collection of the forecasted data for several key parameters related to dust and sand storms in Eastern province of Saudi Arabia.
3. Development of a modified approach to physically model dust and sand storms based on the concept of layering.
4. Suitable conceptual and mathematical support for the modifications done in currently available models.
5. Experimental work pertaining to dust and sand particles size measurements as well as suitable distributions in Saudi Arabia.
6. Design of an enhance model to counter the dust and sand induced weather impairments.

CHAPTER 2

LITERATURE REVIEW

Dust and sand storms are regarded as a serious environmental issue or as a natural disaster. They often arise in deserts and surrounding areas. Consequently, they present an important index of the desertification of land. Some of the famous dust and sand storm occurrence regions include Middle East, Central Asia, North America, Central Africa and Australia. All these regions are connected with severely desertified areas [23].

2.1 Studies of Dust and Sand Storms

The studies on analyzing dust and sand storms have continued for a long time. The characteristics of temporal and spatial dust and sand distributions, average wind speed and other climatic characteristics. related to the dust and sand storms have been discussed in [23], [24]. In the 1980s, the phenomenon of several weather conditions related to dust and sand storms generation was presented in [25]. Similarly, [26] pointed out the maximum frequency of dust and sand storms in Mexico City during the month of March and analyzed the temporal and spatial distributions of such anomalous weather conditions. The occurrence of a dust and sand storm in the trans-atlantic region, based on satellite and GATE data is discussed in [27]. Furthermore, several characteristics pertaining to the raising wind and descending currents for occurrence of such storms have been discussed in [28]. Analysis of several features related to 'Haboob' type dust and sand storms has been presented in [29]. An overview of sources, distributions, frequency and trends of dust and sand storms in China has been highlighted in [30]. Table 2.1 presented the grades of dust and sand storms for different levels of dust intensity, wind speed, and visibility.

Table 2.1: Dust and Sand Storm Grades [31]

Grade	Intensity of Dust and Sand Storm	Instant Extreme Wind Speed (m/s)	Minimum Visibility (m)
1	Severe	≥ 25	< 50
2	Strong	≥ 20	50 – 200
3	Moderate	≥ 17	200 – 500
4	Weak	≥ 10	500 – 1000

2.2 Methodology of Dust and Sand Storms Likelihood

Several meteorological variables such as the cloud cover, relative humidity, surface winds and temperature should be known for optimal prediction of a dust and sand storm [32]. Possibly, many permutations of such variables are associated with the dust and sand storm events. The initiation of a dust and sand storm may be delayed or even prevented due to the presence of sufficient cloud cover. Similarly, various combinations of the underlying environmental parameters may result in a partial or less intense storm. By considering such possibilities, a significant forecast of dust and sand storms can be made.

There is a large variation in the temperature of deserts due to the dry air. Consequently, the dust and sand storms usually subside soon after the sunset because of a swift loss of heat during the night as the strong irradiative cooling tends to lower the inversion and settle the dust [33]. A 20 knot wind may be sufficient to raise dust during the day, whereas during the night it may not be sufficient [33].

The forecast of visibility during a dust and sand storm is very difficult [32]. During a dust haze, the visibility may remain at 5 km to 9 km. Whereas, it may be reduced to almost zero with in and close to the source regions. An increase in visibility is expected while moving away from the source region. The dust and sand particles tend to settle as the wind speed drops below the amount necessary to carry them. During a dry season certain level of dust haze persists almost constantly in the region. Visibility is degraded more due to small particles as compared to the larger ones. But generally, the least visibility occurs within 6 m of the surface [33].

Only the strong wind blows are not a sufficient condition for a dust and sand storm. In fact, to loft the dust and sand particles the wind must blow in a reasonable unstable environment and should be sufficiently turbulent. Information related to diffusion and dispersion of particles, wind speed, turbulence and stability is collectively regarded as the friction velocity. Useful predictions related to the emission of dust and sand can be attained by computations of friction velocity. Many mathematical models weather use this parameter for weather predictions. Navy Operational Global Atmospheric Prediction System (NOGAPS) is a global forecast model being spectral horizontally and energy-conserving finite difference vertically [33]. The NOGAPS friction velocity products are thus very useful for dust and sand forecasts [32], whereas it is not appropriate during vast spread dust and sand storm events as the particles are carried from far distances.

2.3 Dust and Sand Storms Models

Several researches have termed the dust and sand storms as a complicated phenomenon and have proposed different models [6], [24], [34]–[41]. The behavioral and compositional characteristics of dust storms occurring across the globe seem to be somehow uncorrelated, due to the non-uniform soil characteristics along with several other environmental factors. Furthermore, at higher frequencies the severity of weather induced impairments becomes increasingly debilitating [36], [37], [39]. Consequently, the optimal management of satellite dependent resources during the weather anomalous conditions is a tough task.

Several mathematical techniques for dust and sand storm and other weather impairment estimations are available. Whereas, the cumulative strategies for such estimations are not widely available [6], [34], [37], [39], [40]. An elliptical model, while viewing the dust and sand storm event from top has been described in [40]. The ellipse expands rapidly until the peak and then shrinks gradually. Furthermore, authors of [5] have discussed the idea of vertical variation of visibility in a dust and sand storm with reference to height. A vertical path adjustment technique has been presented in [6] according to the characteristics of dust and sand storm. A dust and sand storm is considered to be severe for the visibility less than 50 *m* [31]. The attenuation estimations vary widely across the channel due to the vertical variation of dust and sand particles.

General formulas for electromagnetic wave (EMW) passing through dust and sand particles have been implemented in [42] based on the forward scattering amplitude under Rayleigh approximation. This approximation is used to study the EM scattering due to interaction with dust and sand particles having radii much smaller than that of the incident wavelength. The data pertaining to visibility has been extracted from literature [4], [43], [44] and is physically measured to quantify the effects of such factors on composite attenuation. Note that, dielectric constant values at various frequencies are defined in [4], [43].

There are tight numbers of geosynchronous orbital spaces that could be utilized for a given frequency band, and nearly all orbital openings are represented with current and arranged C-band and Ku-band. So, the Ka-band seems to be a definitive answer for any new satellite correspondence framework. Ka-band has an immense disadvantage in comparison with C-band and Ku-band due to higher frequency range allotment [5], [45]–[48].

2.4 Factors Influencing Dust and Sand Storms

Dust and sand storms are considered as an anomalous weather phenomenon having micro scale storms, which can come in play due to small convections caused by cold air front [49]. The key factors influencing a dust and sand storm event include:

- Atmospheric conditions at air surface.
- Transport of dust and sand particles; i.e. coming in, going back or flowing through.
- Energy balance or diverse i.e. solar radiations intensity and emissions from the ground surfaces under cold and warm air columns.
- The formation of a strong, medium or small scale storm due to vertical convections resulting from the impact of cold air on warm air [6].

2.5 Effects of Dust and Sand Storms

Large volumes of dust and sand can be transported due to these storms unexpectedly. The leading edge of such a storm may be composed of solid wall of dust and sand having 1.6 km height [50]. They impose grave effects on radio wave propagation, i.e. shorter wavelengths observe more attenuation and scattering from particles of dust and sand along the radio path. Loss of signal energy due to encounter with particles along the radio wave propagation path results in service degradation or in severe cases may lead to outage of the communications link. Polarization characteristics of the radio waves are also affected during dust and sand storms, resulting in de-polarization or cross-polarization which may create issue of interference.

Dust and sand particle size also plays an important role in the resultant values of attenuation i.e. for large particles attenuation is high and for small particles the attenuation is low. In fact the signal impairments are maximum when the particles diameter closely corresponds to the signal wavelength. On the other hand, it is very difficult to measure the radius of dust particles and the density of dust in the air. In dust storm, the particle sizes accumulated in air are non-uniform i.e. making a mixture of particles with different radii.

The problem becomes complicated since some authors have claimed that the dust particles size distribution is wind speed dependent [51]–[53] while others reported that the distribution is independent of wind speed [54]. Similarly, more than one distribution may exist during a storm [55]. For each specific condition, measurement and proper fitting of the probable distribution are necessary to achieve accurate impairments prediction [56].

2.6 Enhanced Decision System

Weather conditions have little to no effect upon low operational frequencies. However, the QoS of a satellite network is hardly affected by atmospheric attenuations at reasonably high transmission frequency. The technical solutions pertaining to QoS improvement depend on proper identification, prediction and qualification of the comprehensive impacts of all the constituent impairment factors.

The improvement in SNR as well as system's throughput based on region specific estimations has been analyzed in [57].

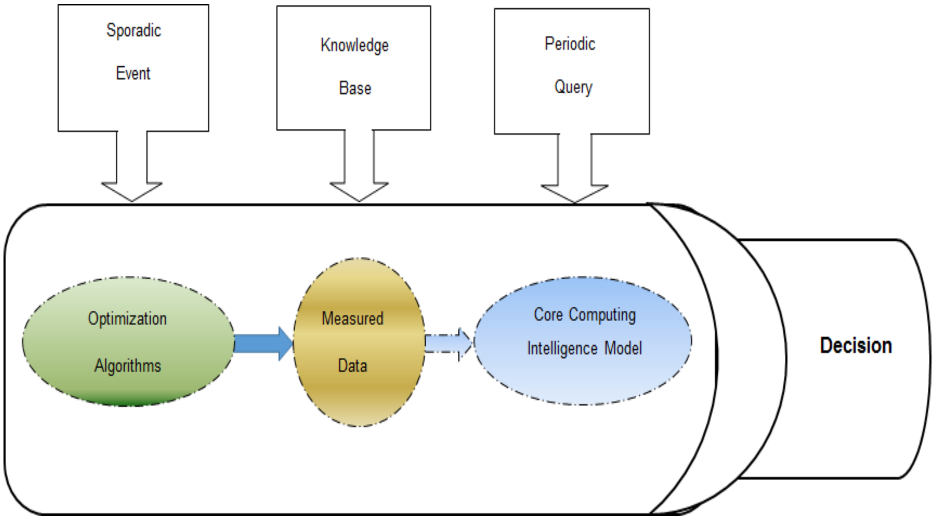

Figure 2.1: Decision Support System (DSS)

By the utilization of a decision support system (DSS) as depicted in Fig. 2.1, the prediction of individual components of satellite networks can be achieved in a cohesive manner. This high level architecture is based on weather attenuation, power, modulation and coding information is used to estimate the optimal decisions for satellite communication systems. This scheme will proficiently search for various combinations of input control variables in order to minimize the estimated attenuation and on the other hand to maximize channel robustness and efficiency by via SNR improvement. Simulation results for SNR with both the estimated and transmitted power are presented in this thesis to show the overall performance improvements.

CHAPTER 3

DUST AND SAND SAMPLES ANALYSIS

This part is related to the study of currently available forecasted environmental parameters and real time measurements of several samples of dust and sand for the eastern province of Saudi Arabia. Since, the dust and sand distribution for different regions is uncorrelated in nature as well as dependent upon the regional surface characteristics, so this data can aid in accurate satellite link impairment estimations due to the frequently occurring dust and sand storms. Consequently, the signal quality can be retained to acceptable levels during the weather deteriorated conditions by incorporating several advance techniques.

3.1 Forecasted Weather Data

The technological improvements in sensory devices and statistical weather analysis have led to the advancement of weather prediction systems. The underlying dust and sand storms related key environmental factors can be forecasted with certain degree of accuracy, which can aid in computation of precise weather induced impairments. In our case, the parameters such as dust and sand concentration level in air, the corresponding variations in visibility, air temperature, wind speed and relative humidity level are available. The aforementioned forecasted factors are sufficient in order to gather preliminary impairment estimations.

Fig. 3.1 and Fig. 3.2 present various forecasted constituent parameters relevant to dust and sand concentration in the atmosphere for the Eastern Province of Saudi Arabia. March and April are usually the months having frequent dust and sand storm conditions. Thus, in order to present a clear view of weather impaired conditions the forecast data was gathered from 9th to 14th of April 2013.

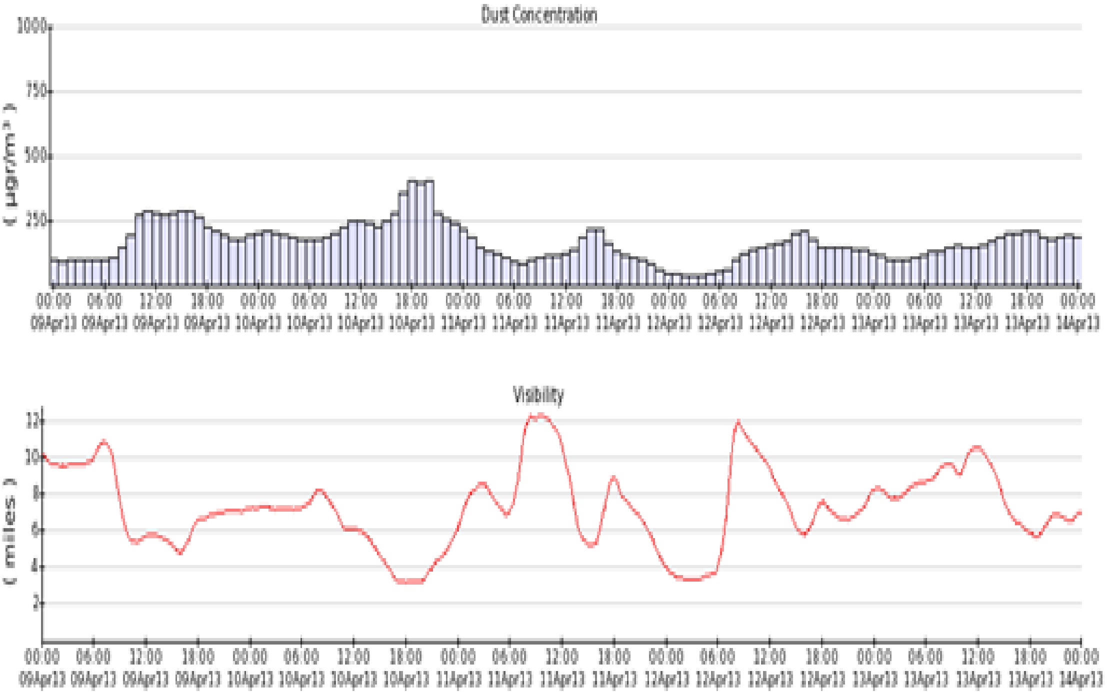

Figure 3.1: Dust and Sand Concentration and Visibility Forecast [10]

According to a study at Center of Excellence for Climate Change Research (CECCR) at King Abdulaziz University, dust particles of very small sizes can remain airborne for 30 days if they attain a height of 1 km and no other vertical accelerations occur. Particles of radius 0.1 to 1.0 μm spend on average 14 days in the atmosphere while particles of 3.0 to 6.0 μm remain elevated for an average of 27 hours.

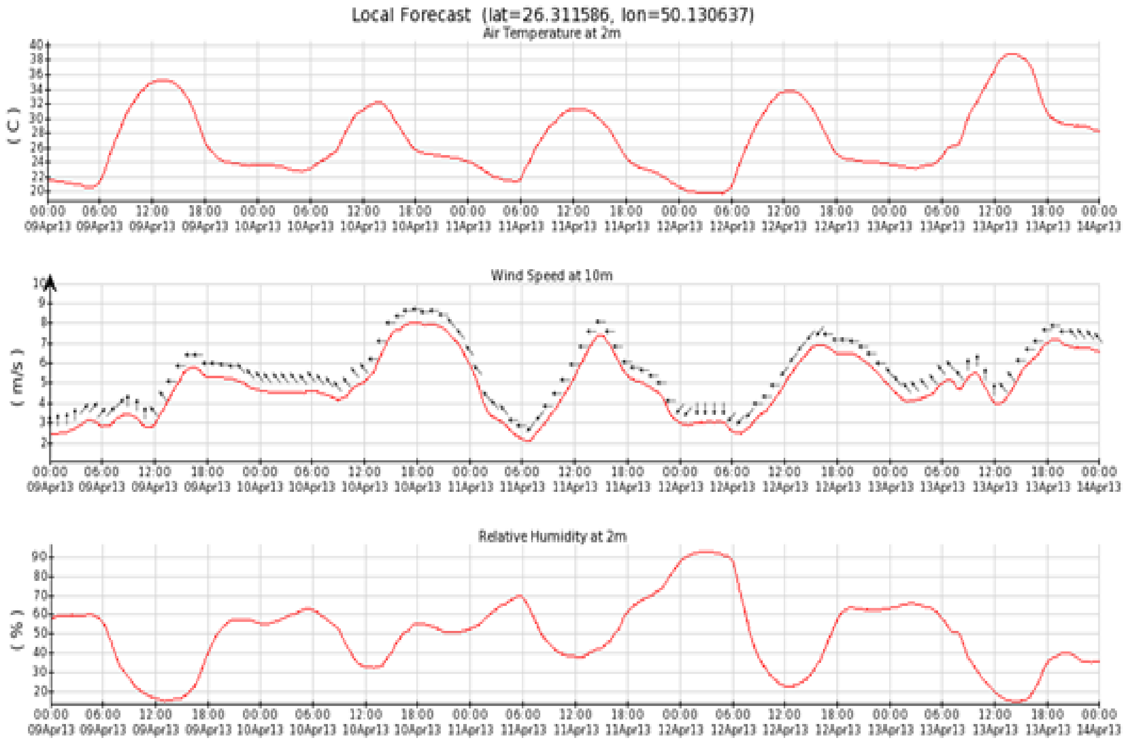

Figure 3.2: Air Temperature, Wind Speed and Humidity Forecast [10]

3.2 Dust and Sand Sample Collections

Furthermore, pertaining to the region specific variation in chemical and physical properties of dust and sand, several experimental details related to particles size distribution have been gathered for samples of Saudi Arabia. Sieve test and hydrometer test have been done on three samples being collected from the open field areas of both developed and undeveloped regions, which can be regarded as the most probable places for initiation and progression of dust and sand storms during July 2013. Each sample weighed approximately 500 grams. Collection sites details are mentioned in Table 3.1.

Table 3.1: Sample Collection Points [1]

Location	Coordinates
Udailiyah (Rural)	25° 8′ 0″ N, 49° 18′ 0″ E
Al-Hassa (Rural)	25° 25′ 46″ N, 49° 37′ 19″ E
Haradh (Urban)	24° 8′ 44″ N, 49° 3′ 55″ E

3.3 Sieve Test

This test was done to measure the dust and sand particles size distribution for acquired samples. The procedure involved a nested column of sieves with wire mesh cloth. The mechanical or sieve analysis is performed to determine the distribution of the coarser, larger-sized particles. This experiment was performed on collected dust and sand samples in September 2013 at Highway Laboratory - Civil Engineering Department in KFUPM. The minimum mesh scale in experiment was 37 μm. Fig. 3.3 shows percentage dust and sand particles distribution for all samples. The rural samples contained a maximum dust particle size of approximately 0.60 mm whereas, the urban sample contained largest particle size of approximately 1.20 mm.

3.3.1 Experimental Setup

This test required a set of sieves having different scales of mesh cloth, a balance machine to weigh the samples masses collected on different sieves, a sieve shaker and a cleaning brush. The test procedure involves following steps,

1. The weights of all sieves and the bottom pan to be used in analysis should be noted.
2. The weights of all the individual dust and sand samples should be recorded.
3. Clean all the sieves before proceeding with the analysis.
4. Arrange them such that the largest size grating sieve is placed at the top and lowest at the bottom.
5. The pan should be placed underneath the last sieve.
6. Carefully pour the dust and sand sample into the sieve at top and put the sieve cover.
7. Place the array of sieves into the shaker and shake for approximately 10 *min*.
8. Now carefully weigh the retained weight of dust and sand sample at each sieve as well as the pan.
9. Finally, record the weight distribution data of dust and sand particles on each sieve.

Fig. 3.3 and Fig. 3.4 illustrate the sieve analysis setup, including the sieves arrangement, weighing mechanism and dust and sand samples shaking procedure.

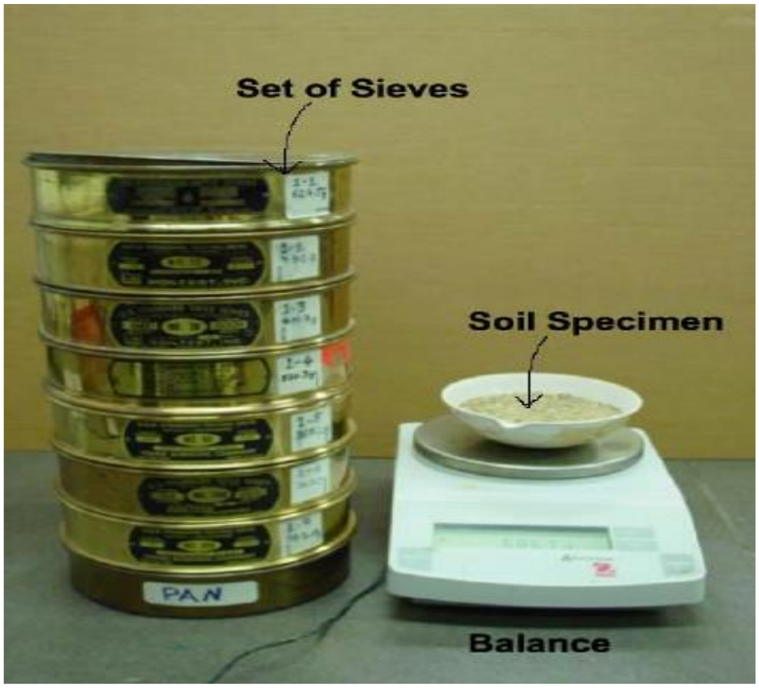

Figure 3.3: Sieve Array and Balance [11]

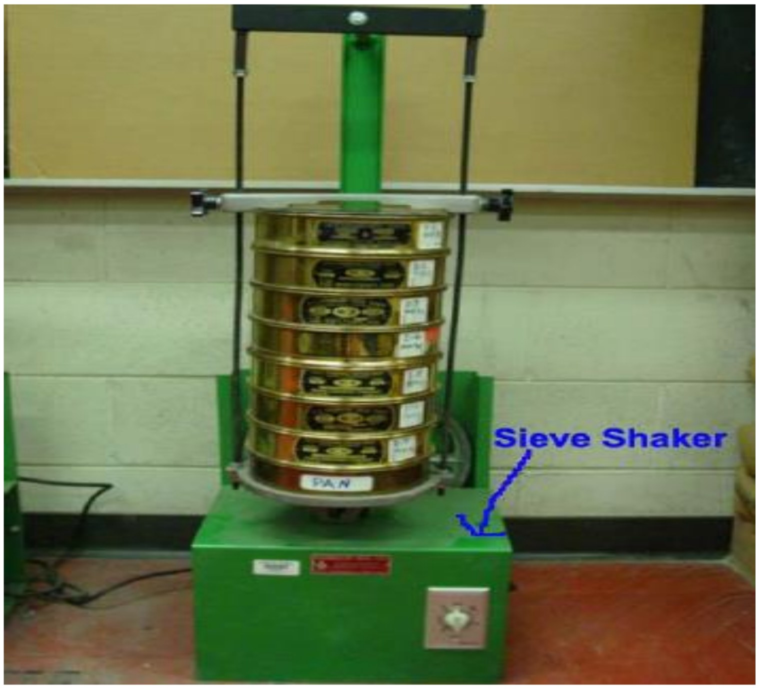

Figure 3.4: Sieve Shaker [11]

3.3.2 Sieve Analysis Details

Further details related to this test have been tabulated in Table 3.2. It is evident from the gathered data that dust and sand particles with approximate sizes of 150 µm have the highest concentration in rural samples i.e. 61.73% and 64.42% respectively, whereas the urban sample has a slightly uniform distribution for all dust particles sizes.

Table 3.2: Sieve Analysis Data

Sieve Size	**Sample 1**		**Sample 2**		**Sample 3**	
	Udaliyah (Rural Area)		**Al-Hassa (Rural Area)**		**Haradh (Urban Area)**	
Micron (µm)	*Weight. Retained (gm)*	*Accumulated Percentage*	*Weight Retained (gm)*	*Accumulated Percentage*	*Weight Retained (gm)*	*Accumulated Percentage*
1180	0.00	0.00	0.00	0.00	2.20	0.44
600	3.30	0.66	2.70	0.54	103.3	20.67
300	122.0	24.37	106.6	21.43	137.6	27.54
150	309.0	61.73	320.5	64.42	93.20	18.65
75	61.50	12.28	64.60	12.99	103.6	20.73
38	3.80	0.76	2.50	0.50	51.00	10.21
<38	1.00	0.20	0.60	0.12	8.80	1.76
	500.6	100.0	497.5	100.0	499.7	100.0

The particles with sizes ≥ 600 μm have been omitted from simulations because they showed 0.44% accumulation only for the urban sample and 0% accumulation for both rural samples. Furthermore, the particles with sizes in this range are not expected to get suspended at high altitudes. Thus there are no degrading effects on the communication link due to particles with sizes ≥ 600 μm. The presented average computation includes uniform averaging for both rural samples as well as the urban sample. Fig. 3.5 and Fig. 3.6 depict the individual and average distributions of dust and sand particles.

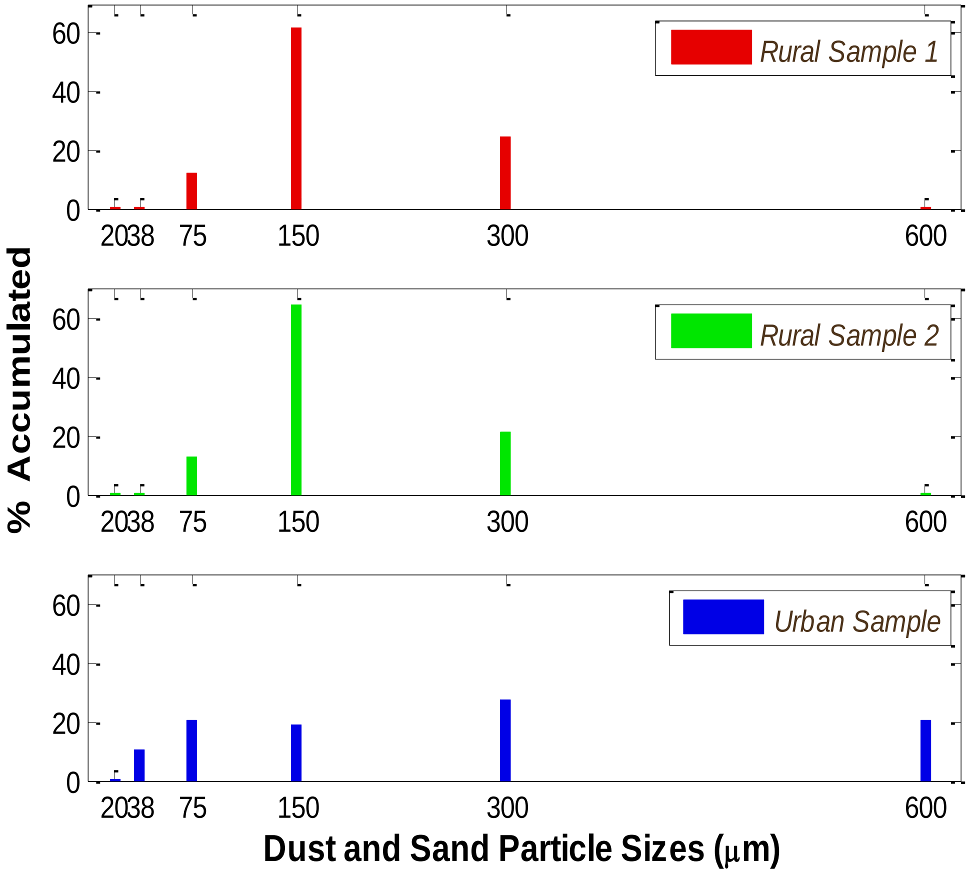

Figure 3.5: Sieve Analysis - Individual Dust and Sand Particles Size Distribution

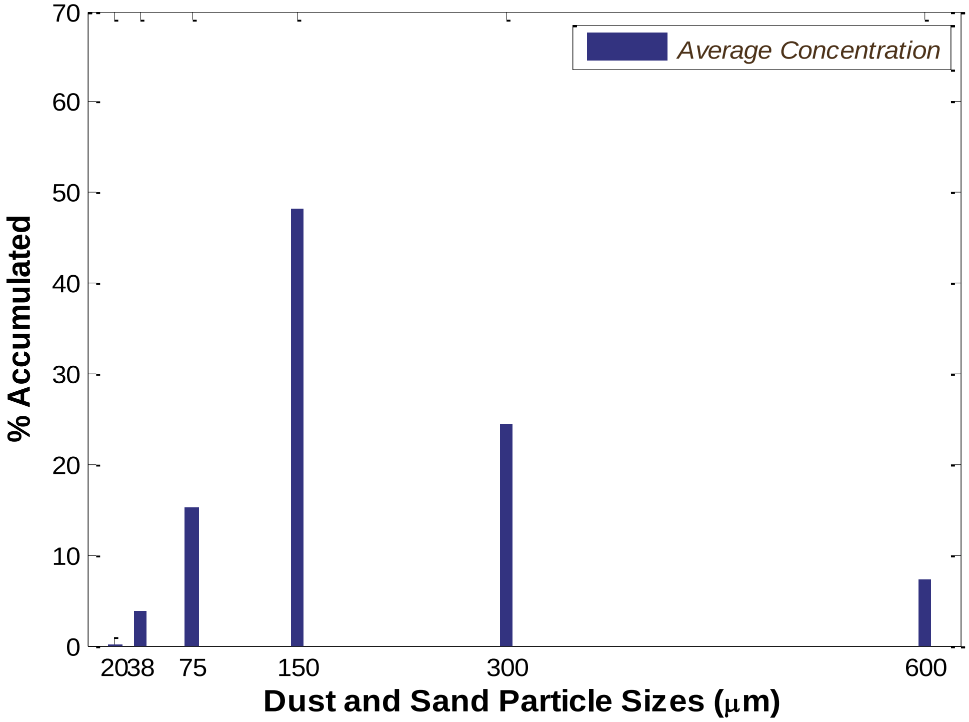

Figure 3.6: Sieve Analysis - Average Dust and Sand Particles Size Distribution

3.4 Hydrometer Test

The hydrometer analysis is used to determine the distribution of the finer dust particles. Since, the minimum detectable dust particles size in sieve test was 37 μm. So, hydrometer test was performed to precisely measure the distribution for smaller sized particles. Although, all the samples showed negligible concentration below 37 μm. But to gather precise details of dust particles size distribution from 1 μm to 37 μm, this test was applied on fine dust of urban sample in September 2013 at Highway Laboratory - Civil Engineering Department in KFUPM, which had 8.80 grams of fine dust particles retained in the lowest pan of sieve analysis.

3.4.1 Experimental Setup

This test required a hydrometer, sedimentation cylinder, control cylinder, blender, thermometer and beaker. The test procedure involves following steps,

1. Collect the fine dust sample accumulated in the bottom pan of the sieves array.
2. Put it into a beaker and add 125 *ml* of the dispersing agent.
3. Stir the mixture making the sample thoroughly wet and let it soak for a minimum of ten *min*.
4. Simultaneously, fill the control cylinder up to the mark with distilled water and put the same amount of dispersing agent.
5. Note readings at the top of meniscus formed by the hydrometer stem and control solution.
6. Note the zero correction and temperature respectively, after inserting the hydrometer into the control cylinder.
7. Collect the soil slurry into a mixing cup by adding distilled water as necessary, until the mixer is at least half full.
8. Shake the solution for almost two *min*.
9. Put the soil slurry into the empty sedimentation cylinder immediately and add distilled water up to the mark.
10. Put a stopper at the open end of cylinder and secure it with the palm of your hand and start turning the cylinder upside down and back upright for almost 1 *min* to thoroughly distribute fine dust particles in the solution.
11. Put the cylinder down and record the time. Remove the stopper from the cylinder.

12. Now for the first reading, insert the hydrometer very slowly and carefully into the solution after 1 *min* and 40 *sec*.
13. Note the reading by observing the top of meniscus formed by the suspension and the hydrometer stem.
14. Now, slowly remove the hydrometer and put it back into the control cylinder.
15. Spin the hydrometer very gently to remove any particles that may have adhered to its surface.
16. Note the readings after 2, 5, 8, 15, 30 and 60 *min*.

Fig. 3.7 and Fig. 3.8 illustrate the experimental setup, including the placement of hydrometer in the control cylinder, specimen preparation for analysis and the sedimentation cylinder.

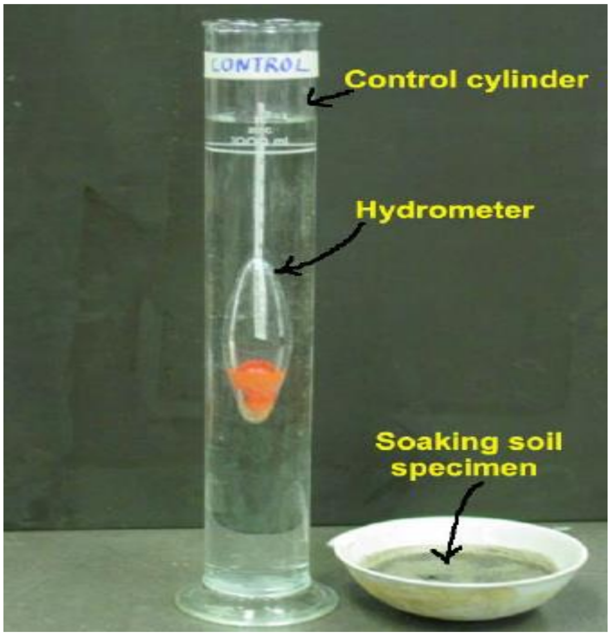

Figure 3.7: Hydrometer, Control Cylinder and Specimen [11]

Figure 3.8: Sedimentation Cylinder – on Left Side [11]

3.4.2 Hydrometer Analysis Details

Further details related to this test have been tabulated in Table 3.3 whereas, the simulation results in Fig. 3.9 shows the dust particles distribution from 1.00 to 40.0 μm.

Table 3.3: Hydrometer Analysis Data

$Micrometers$ (µm)	$Proportion$ ($Percentage$)
> 40	0
40-21	40.5
20-11	35.3
10-01	15.6
<1	8.6

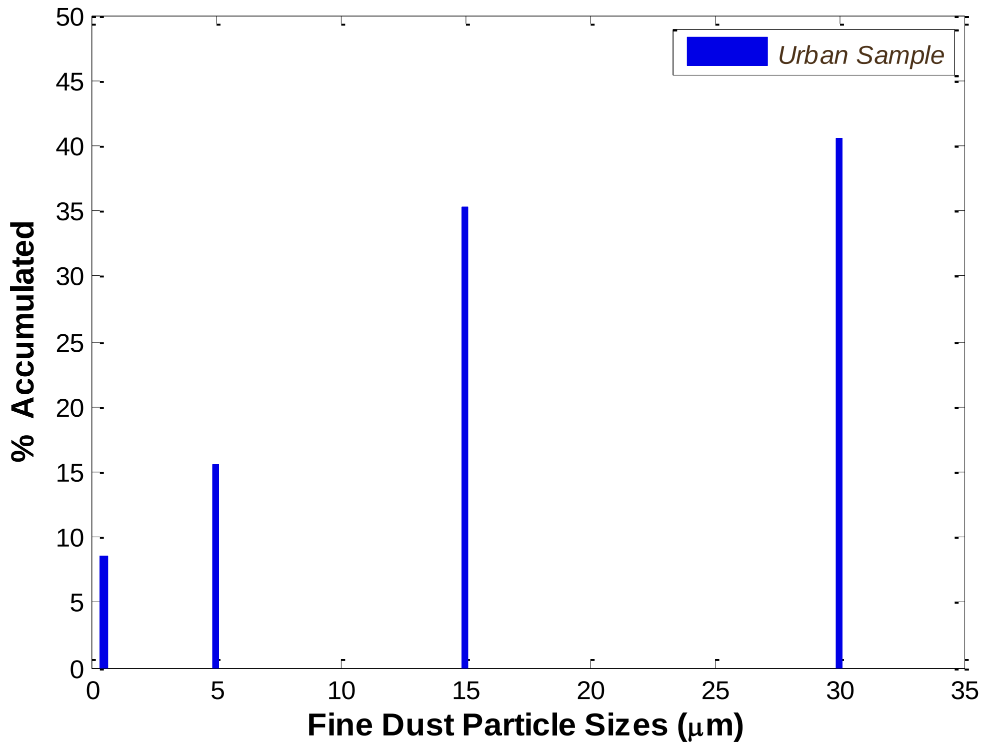

Figure 3.9: Hydrometer Analysis - Fine Dust Particles Size Distribution

3.5 Visibility Measurements during Dust and Sand Storms

A satellite earth station was installed in September 2012 at KFUPM to analyze the impairments resulting from dust and sand storms. Several signal quality parameters readings were taken at different times. In clear weather the maximum received signal quality attained was approximately 80%, whereas the readings taken during dust and sand storms conditions, the signal quality degraded to approximately 50%.

During a signal quality estimation activity being performed in April 2013, the optical visibility was also measured as presented in Fig. 3.10 and Fig. 3.11. The visibility level depicted in depicted cases is expected to be around 500 *m* and has been incorporated in the simulated estimations presented in Chapter 4.

Figure 3.10: Visibility Estimation – I

Figure 3.11: Visibility Estimation - II

Due to the uncorrelated nature of dust and sand particles for different regions of world, the samples for Saudi Arabia region were analyzed. The analysis details related to assumed as well as real time dust and sand particles measured distributions gathered from the sieve and hydrometer tests have been utilized in the simulation work presented in subsequent parts of this work, which is expected to closely approximate the constituent impairments due to dust and sand storms occurring in Saudi Arabia.

CHAPTER 4

IMPAIRMENTS ESTIMATION METHODOLOGY

Literature pertaining to dust and sand storms effects on satellite signals has been thoroughly reviewed and a novel approach is devised to physically and mathematically model such weather anomalous conditions. The previous section deals with experimental details related to dust and sand particles sizes and distribution, level of visibility, just to name a few key parameters for impairments estimation.

The dust and sand storms show uncorrelated behavior for different regions of world. So, the data available in literature as well as the information collected from real time measurements of dust and sand samples is utilized in this chapter for proper quantification of attenuation due to dust and sand storms in Saudi Arabia.

4.1 Significance of Visibility Estimation

A mathematical strategy for dust and sand impairments estimation can be initiated by the computation of visibility at certain reference height during the weather impaired conditions. The value of visibility varies with respect to height with in a dust and sand storm. Therefore, accurate measurement of the visibility can be done by means of a visibility sensor. Based on the statistical data visibility in Khartoum over a period of 5 years from 1975 to 1980 for an earth station to satellite link operating at 10 GHz, (4.1) depicting the relation of visibility to height has been devised in [12];

$$V = V_o \left[\frac{h}{h_o}\right]^{0.26} \qquad h_o \le h \le h_l \tag{4.1}$$

where visibility (V) at any height (h) can be related to the visibility (V_o) at a reference height (h_o) and h_l is the maximum height of dust and sand storm. It should be noted that the all the mathematical expressions are valid only for the dust and sand filled region i.e. $h_o \le h \le h_l$.

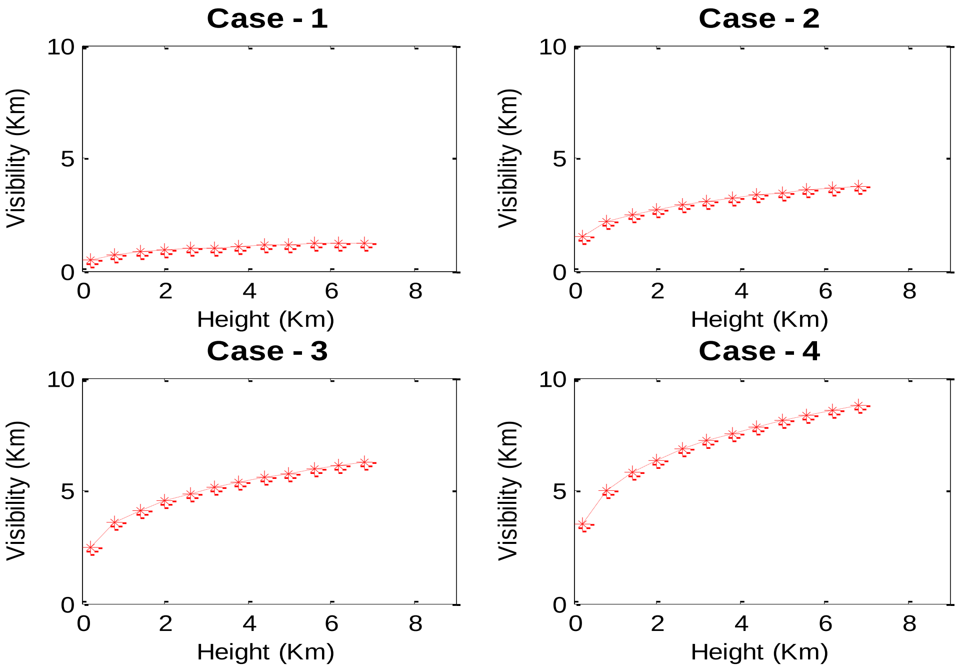

Figure 4.1: Visibility Variation Cases

Fig. 4.1 presents four distinct cases for depicting the degree of variations in visibility with respect to height with in a dust and sand storm. The visibility at $h_o = 0.2\ km$ is increased by 1 km in each case i.e. starting from 0.5 km in case 1 to 3.5 km in case 4, whereas the total height of dust and sand storm is considered to be approximately 7 km, for all the depicted scenarios.

Details related to visibility clearly depict the significance of accurate visibility quantification during the dust and sand storms in order to gather precise attenuation estimates. In case 1, starting from 0.5 *km* visibility and after traversing almost 7 *km* in the dust and sand filled region 1.25 *km* visibility is attained. On the other hand, in case 4 visibility significantly increases from 3.5 *km* to 8.75 *km*. Therefore, in order to be precise with impairment estimations, the altitude based non-uniformity of several dust and sand parameters is taken into account. Table 4.1 shows the minimum visibility (V_{min}) and maximum visibility (V_{max}) estimates for each case of Fig. 4.1.

Table 4.1: Different Scenarios for Visibility Variation

Cases	$\boldsymbol{V_{min}}$ *(km)*	$\boldsymbol{V_{max}}$ *(km)*
1	0.5	1.25
2	1.5	3.75
3	2.5	6.25
4	3.5	8.75

4.2 Visibility Layers

On the basis of variations in level of visibility, a strategy is devised to present the dust and sand storms physically. The model is composed of horizontal layers with respect to visibility. Furthermore, the distance traversed by radio wave in the dust and sand filled region is regarded as the slant path (L) *km*, which is subdivided into n visibility dependent slant patches or layers $L_1, L_2, \dots, L_{n-1}, L_n$ with their respective heights $h_1, h_2, \dots, h_{n-1}, h_n$.

Each slant patch (L_i) contains its own parameters of dust impairments such as dust and sand particles concentration, their average sizes and visibility levels. The total number of slant patches can be selected according to a scheme consistent in all the subsequent computations while providing a reasonable variation in visibility.

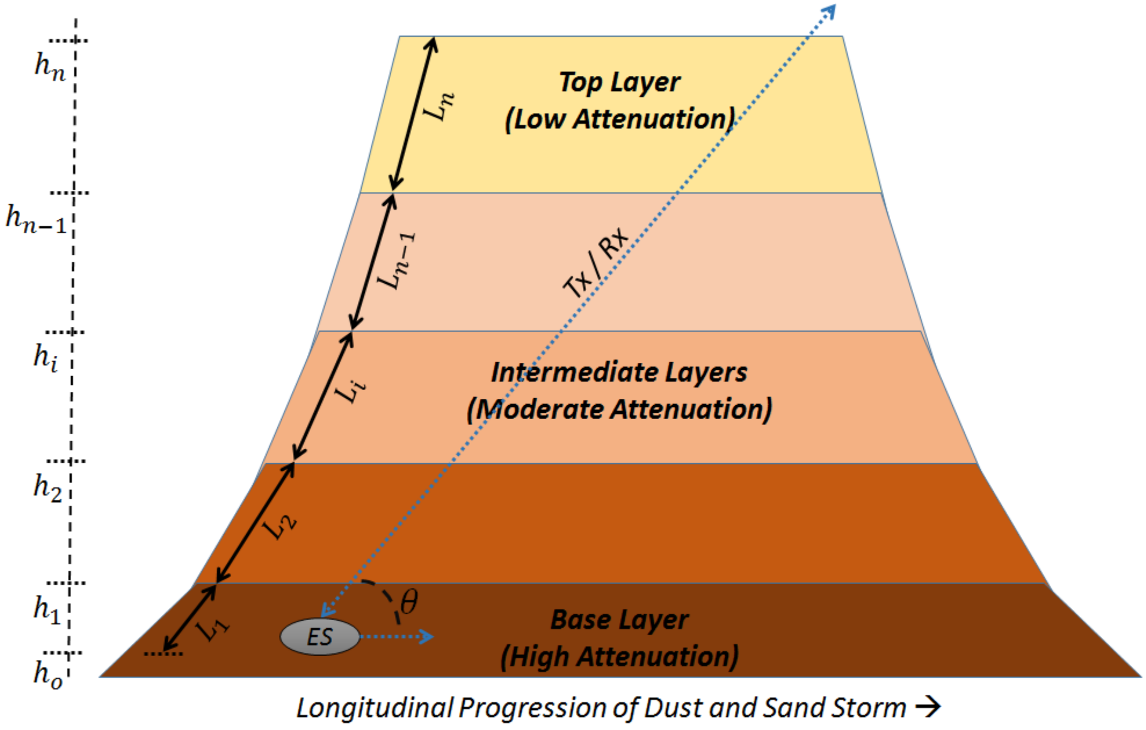

Figure 4.2: Dust and Sand Storms Layered Model

The physical scenario in Fig. 4.2 illustrates an earth station *(ES)* located in a dust and sand storm effected region. The transmit *(Tx)* and receive *(Rx)* signals passage through radio channel occurs at an elevation angle (θ). Furthermore, the lower level layers impose more attenuation as compared to the upper order layers, due to greater concentration and larger diameters of dust and sand particles.

4.3 Layering Scheme

High concentration of dust and sand particles within storm ultimately leads to low visibility, thus inducing more wireless channel attenuation. Thus a strategy is devised to make visibility dependent horizontal layers of the dust and sand storms, based on the indirect relation between visibility and attenuation.

Table 4.2: Layers Boundaries Chart

Slant Patch / Layer	$\boldsymbol{V}$ *(km)*	$\boldsymbol{h}$ *(km)*
L_1	$V_0 \leq V \leq V_1$	$h_0 \leq h \leq h_1$
L_2	$V_1 \leq V \leq V_2$	$h_1 \leq h \leq h_2$
L_i	$V_{i-1} \leq V \leq V_i$	$h_{i-1} \leq h \leq h_i$
L_{n-1}	$V_{n-2} \leq V \leq V_{n-1}$	$h_{n-2} \leq h \leq h_{n-1}$
L_n	$V_{n-1} \leq V \leq V_n$	$h_{n-1} \leq h \leq h_n$

Thus, in the first layer (L_1) visibility varies from V_0 to V_1 and the width can be computed by subtracting the initiation point of second layer from the initiation point of previous layer i.e. $(h_1 - h_0)\ km$. Similarly, the subsequent layer visibilities and widths can be obtained from Table 4.2. The slant path (L_i) traversed by radio wave in i^{th} layer can be computed from (4.2):

$$L_i = (h_i - h_{i-1})\ sin\theta \tag{4.2}$$

Furthermore, L_n is the top layer containing a low concentration of dust and sand particles after its boundary the mathematical formulas for dust and sand storm impairments models are not applicable. So, either free space losses *(FSL)* should be computed or another weather anomalous model should be applied. Similarly, (4.3) is obtained in [5] after interchanging the parameters of (4.1) and introducing the layers indexing parameter *(i)*:

$$h_i = h_{i-1} \left[\frac{V_i}{V_{i-1}}\right]^{3.85} \qquad 0 \leq i \leq n \tag{4.3}$$

where h_i is starting height of i^{th} layer and V_i is the reference visibility in that layer. Similarly, h_{i-1} and V_{i-1} are the previous layer's height and visibility and i is an index parameter whose value can be chosen after deciding the total number of layers for a particular dust and sand storm scenario.

Equation (4.3) is computed in a recursive manner such that if the value of visibility (V_{i-1}) in a particular layer increases from the visibility threshold defined for that layer (L_{i-1}) at height (h_{i-1}), it is regarded as the initiation of a new layer (L_i) with visibility (V_i) and height (h_i).

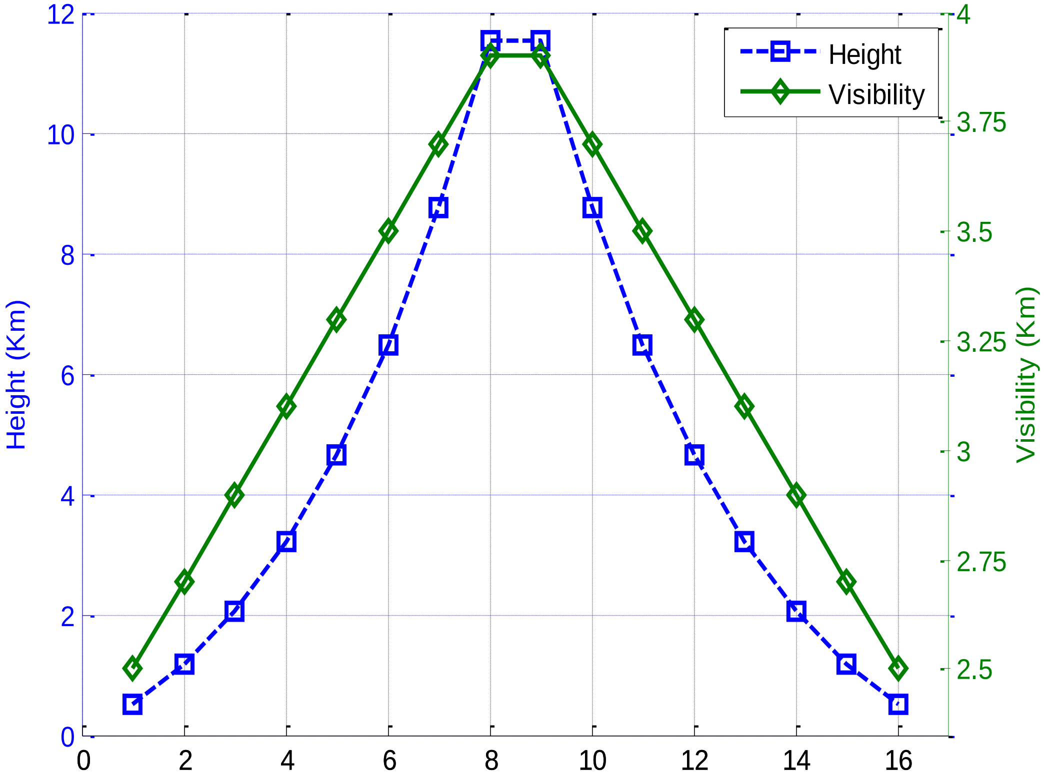

Figure 4.3: Dust and Sand Storm Mirrored Model with Visibility & Height Variations

Fig. 4.3 presents a seven layered dust and sand storm simulation with monotonic increase in visibility with respect to height assuming symmetric conditions. The initial height (h_o) is 500 *m* and the corresponding visibility (V_o) is 2.5 *km*. In this case each 200 *m* increase in visibility from the reference value is considered as a new layer of dust and sand storm. The diamonds (◊) represent initiation of new layers and the boxes (□) denote the corresponding heights or start points of each layer in upwards direction. The maximum height of layers in the presented scheme is 11.5 *km*.

4.4 Dust and Sand Particles Size Variations

Dust and sand particles size distribution assessment is very important for predicting the overall impairment effects of storms. Each dust and sand storm may have totally uncorrelated dust distributions. Moreover, this distribution is also dependent on height. Degradations in visibility occur due to high concentrations of dust and sand particles in the air. The radio wave would strike with a lot of such particles before leaving the dust filled region. Hence, the well-known phenomenon of wave energy absorption and scattering occurs along with depolarization leading to greater radio wave impairments.

At higher altitudes within a storm the average diameter of particles decreases because the heavier dust particles have greater fall velocities as compared to the particles with smaller sizes that remain suspended in the air for longer intervals of time. An inverse relation exists between dust particles average sizes (D_{avg}) and height (h), as discussed in [58]. The relation between average diameter D_{av} and height h is represented by [24]:

$$D_{av} = D_o\, h^{-\alpha} \tag{4.3}$$

where $\alpha = 0.155$.

Assuming the circular geometry for dust and sand particles, the equivalent or average particles radius (r_{eq}) can be computed as:

$$r_{eq} = {}^{D_{av}}\!/_{2} \tag{4.4}$$

Freeman's chain code algorithm was incorporated in (4.3) and (4.4) for including the dust and sand particles of nearby sizes for better estimates. This estimation provides an enhanced result under light and medium dust and sand storms, where the particle sizes are assumed to be uniformly distributed. Therefore, in case of severe dust and sand storm scenarios other assumptions should also be considered to achieve reasonable outcomes.

4.5 Dust and Sand Dielectric Constants

Several researches have estimated the real and imaginary parts of dielectric constants (ϵ' and ϵ'') of dust and sand particles for different types of soil and specific ranges of satellite operation frequency. Dielectric constant values are presented in Table 4.3.

Table 4.3: Dielectric Constants for Various Soil Types [38], [59], [60]

$\boldsymbol{Frequency\ (GHz)}$	$\boldsymbol{Soil\ Type}$	$\boldsymbol{\epsilon'}$	$\boldsymbol{\epsilon''}$
$1-3$	$Loam$	3.5	0.14
$3-10.5$	$Clay, Slit$	5.73	0.474
$10.5-14$	$Sand$	3.9	0.62
$14-24$	$Sand$	3.8	0.65
$24-37$	$Loam$	2.88	0.3529

4.6 Impairments Estimation

Point attenuation (A_p) is the dust and sand impairment induced in *dB/km* whereas, dust attenuation (A_D) is the total impairment due to radio wave propagation in the dust and sand covered region. Each layer constitutes its specific A_p at the microwave signal depending on the measure of visibility and the equivalent dust and sand particles equivalent radii in that particular layer. These individual layered attenuations are then summed up till the end of dust and sand storm. The clear air conditions can be assumed upon attaining a certain lower bound of visibility as observed in the clear weather conditions [5], [34], [39]. The expression for point attenuation is presented in [6]:

$$A_p = \left[\frac{5.67 \times 10^2}{V\, r_{eq}^2\, \lambda}\right] \left[\frac{\varepsilon''}{(\varepsilon' + 2)^2 + \varepsilon''^2}\right] \sum_i p_i r_i^3 \tag{4.6}$$

where r_{eq} is equivalent dust particle radius, λ wavelength, ε' and ε'' are real and imaginary parts of dust dielectric constant and $\sum_i P_i r_i^3$ is the summation of particle sizes probability between r_i and $r_i + \Delta r_i$ times its volume.

Similarly, the expression for evaluating the total impairments induced in *dB* due to dust and sand storms is given in [5], [34], [39]:

$$A_D = r_v \times \sum_{i=0}^{n} L_i\, A_p \tag{4.7}$$

where r_v is the vertical patch adjustment factor, L_i is the width of i^{th} layer.

Dust and sand particle sizes and the corresponding distributions also play a pivotal role in accurate quantification of imposed impairments. Therefore, three different scenarios including the uniform distribution, normal distribution and experimental analysis of the dust and sand are presented in this section. Afterwards, the expected impairments due to each distribution on the radio waves are evaluated based on the mathematical models described in [1], [3], [5].

The proposed model takes into account three different dust and sand particles distributions along with varying visibility and particles sizes, to compute their respective attenuations for a wide range of frequencies.

4.6.1 Uniform Distribution

The uniform distribution of dust and sand particles radii with a mean of 50 μm has been illustrated in Fig. 4.4. This distribution has been utilized in order to estimate the dust and sand impairments effects from (4.5) and (4.6). The particles range from 20 μm to 80 μm.

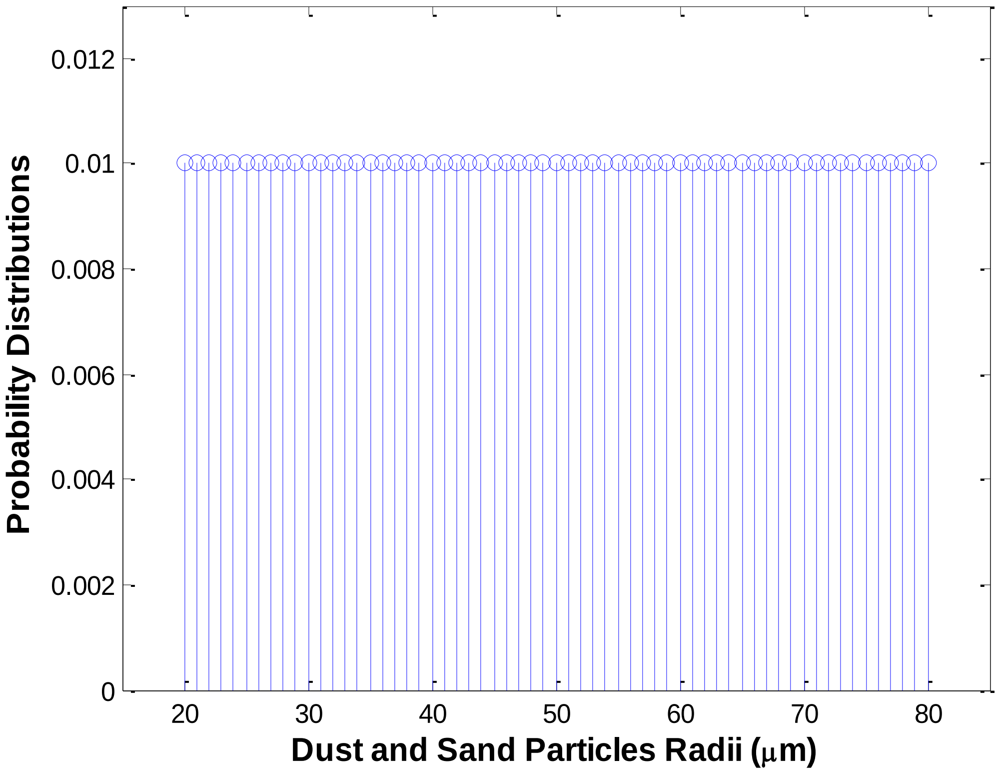

Figure 4.4: Discrete Uniform Distribution for Dust and Sand Particles

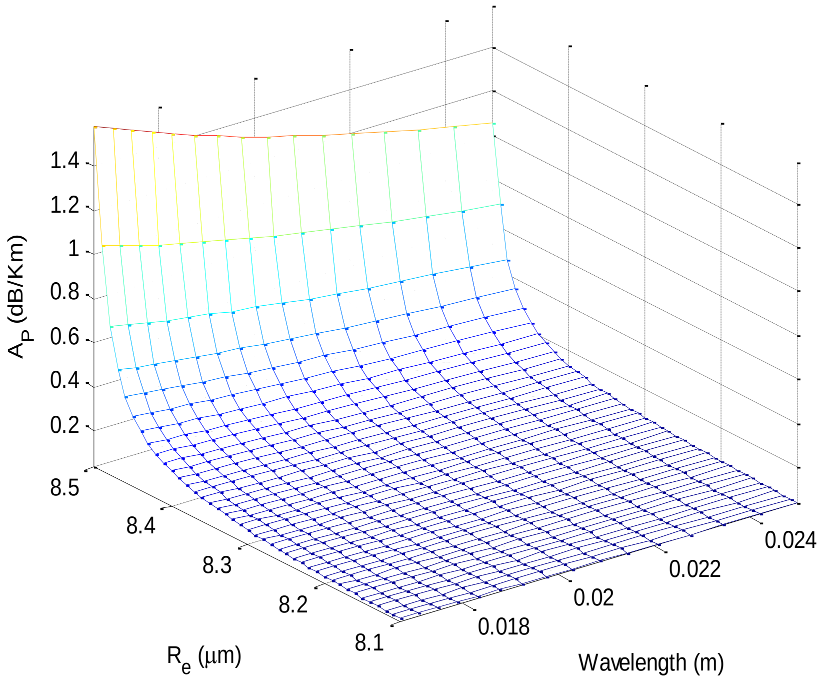

Figure 4.5: Point Attenuation for Uniform Distributed Dust and Sand Particles

The three dimensional plot in Fig. 4.5 presents point attenuation estimates for uniform distribution of dust and sand particles radii (R_e) along with variation in radio frequency. A peak of almost 1.5 *dB/km* dust and sand induced impairment is expected in this scenario. Similarly, Fig. 4.6 presents the total dust attenuation expected due to the uniform distribution based on the quantifications from (4.7). In this case approximately 4.5 *dB* of total dust and sand impairment is expected on the satellite and earth station link operating in the Ku band.

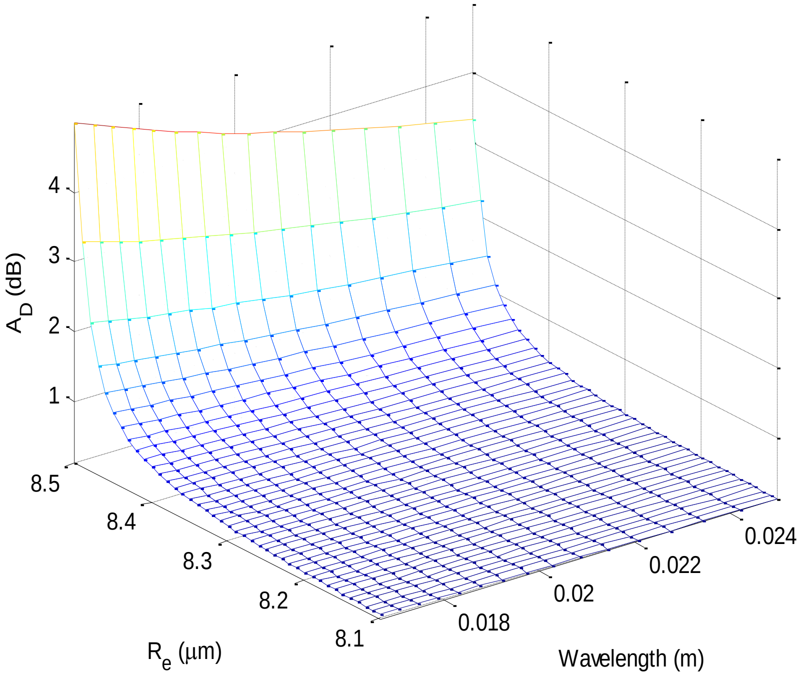

Figure 4.6: Dust Attenuation for Uniform Distributed Dust and Sand Particles

4.6.2 Normal Distribution

The normal distribution of dust and sand particles radii with a mean of 50 μm and variance of 15 μm have been illustrated in Fig. 4.7. In this case the dust and sand particles radii range from 1.00 μm to 100 μm. This particles radii distribution data presented in Fig. 4.7 has been utilized in order to estimate the dust and sand impairments effects from (4.5) and (4.6).

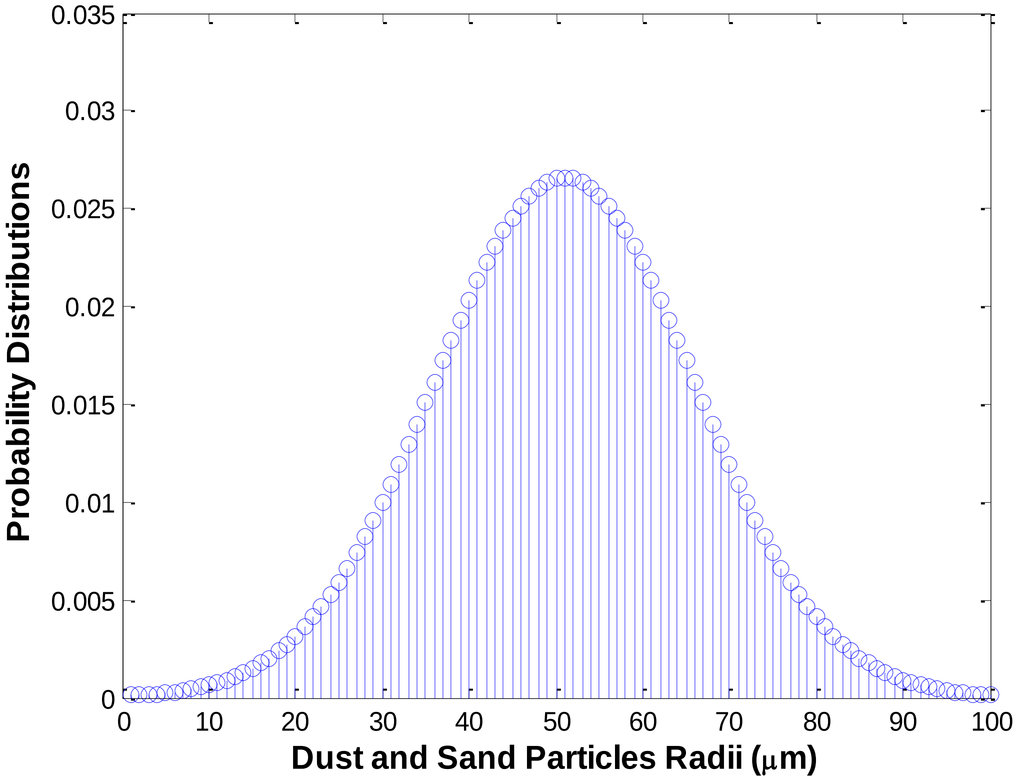

Figure 4.7: Discrete Normal Distribution for Dust and Sand Particles

The three dimensional plot in Fig. 4.8 presents point attenuation estimates for normal distribution of dust and sand particles radii along with variation in radio frequency. A peak of almost 1.7 *dB/km* dust and sand induced impairment is expected in this scenario. Similarly, Fig. 4.9 presents the total dust attenuation expected due to the normal distribution based on the quantifications from (4.7). In this case approximately 5.2 *dB* of total dust and sand impairment is expected on the satellite and earth station link operating in the Ku band.

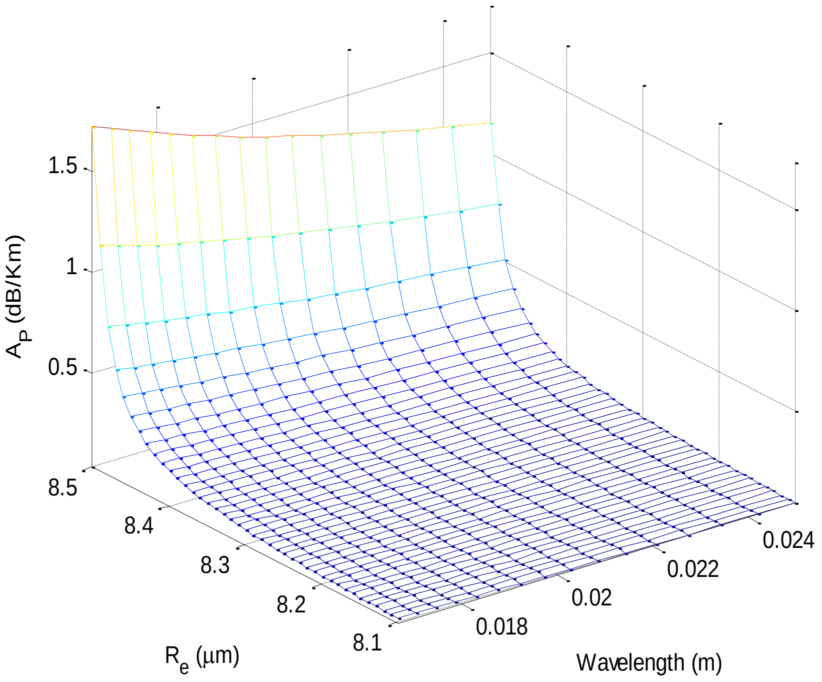

Figure 4.8: Point Attenuation for Normal Distributed Dust and Sand Particles

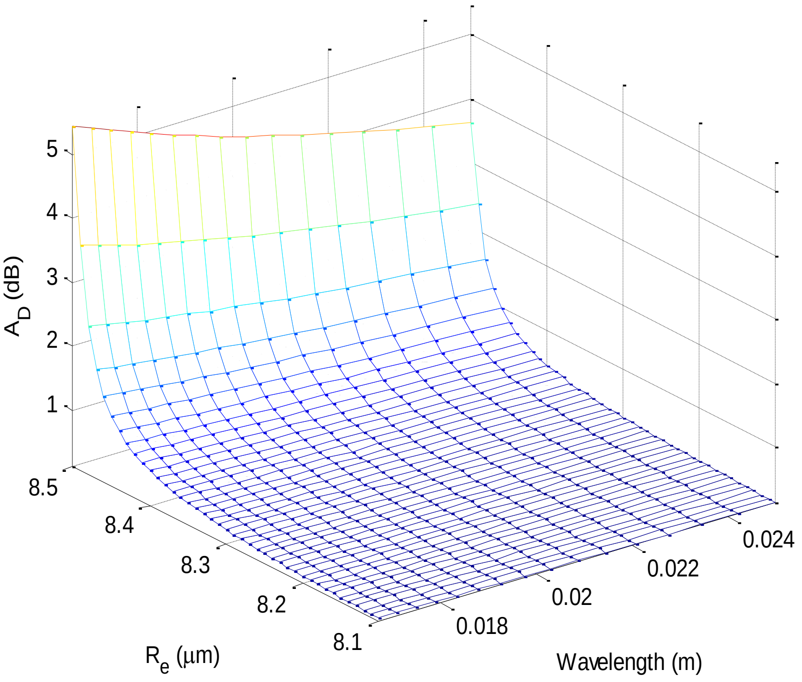

Figure 4.9: Dust Attenuation for Normal Distributed Dust and Sand Particles

4.6.3 Analyzed Distribution

The analyzed dust and sand particles radii distribution have been illustrated in Fig. 4.10. Sieve and Hydrometer tests were performed in order to get these details. The circular geometry for dust and sand particles is considered for getting the equivalent radii from the dust and sand particles sizes. The peak of approximately 45% particles of 75 μm radius were observed from the real time measurements. In this case the dust and sand particles radii range from 1.00 μm to 150 μm has been shown. The particles radii distribution data presented in Fig. 4.10 has been utilized in order to estimate the dust and sand impairments effects from (4.5) and (4.6).

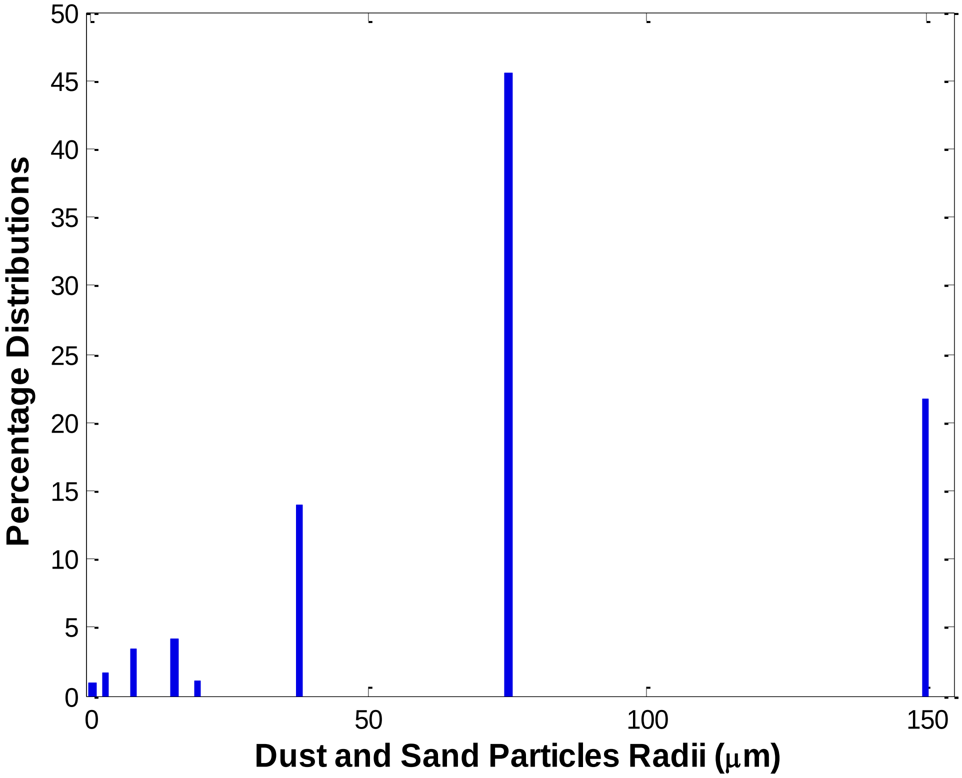

Figure 4.10: Analyzed Distribution for Dust and Sand Particles

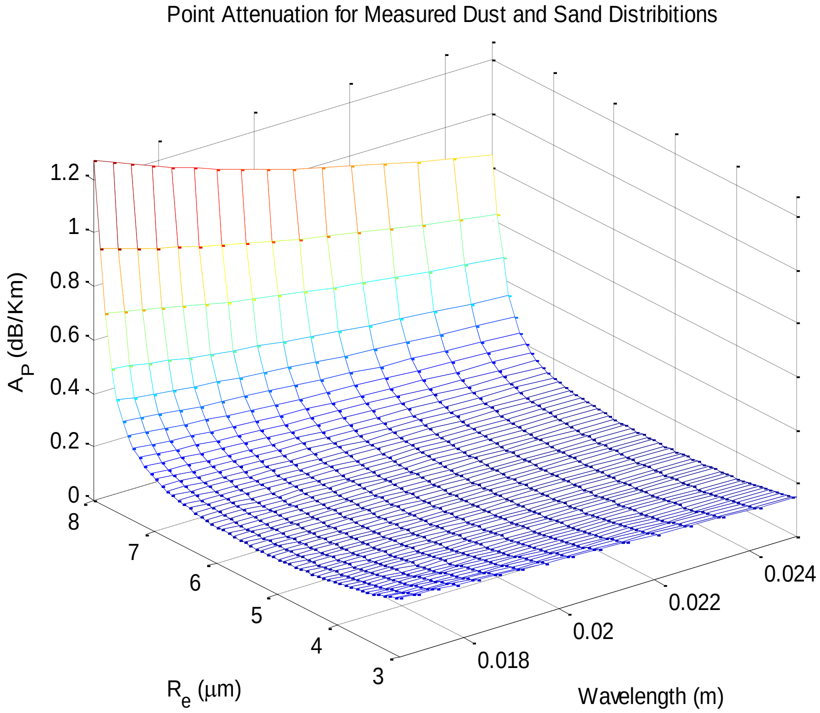

Figure 4.11: Point Attenuation for Measured Dust and Sand Particles Distribution

The three dimensional plot in Fig. 4.11 presents point attenuation estimates for analyzed distribution of dust and sand particles radii along with variation in radio frequency. A peak of almost 1.3 *dB/km* dust and sand induced impairment is expected in this scenario. Similarly, Fig. 4.12 presents the total dust attenuation expected due to the normal distribution based on the quantifications from (4.7). In this case approximately 3.2 *dB* of total dust and sand impairment is expected on the satellite and earth station link operating in the Ku band.

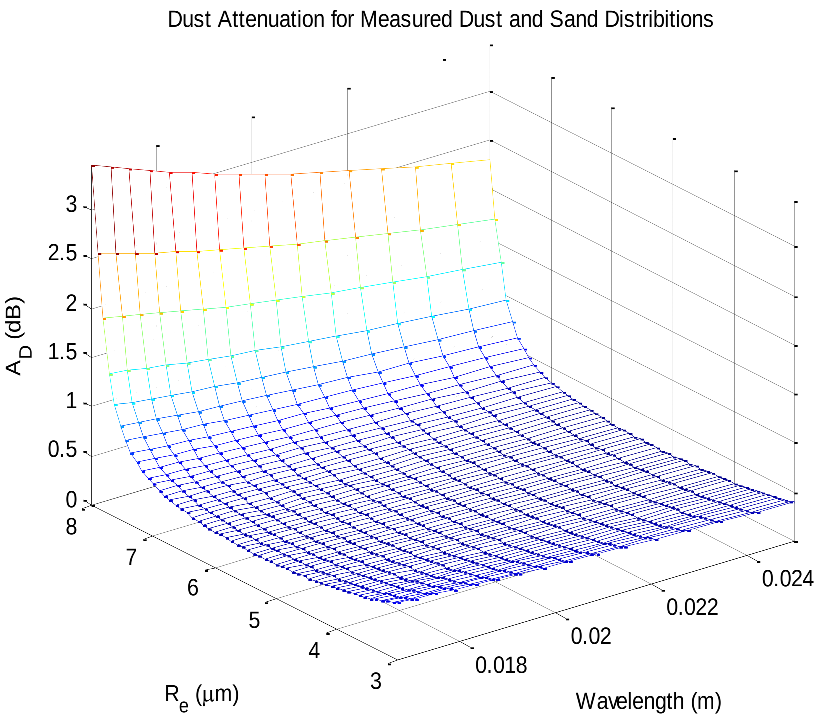

Figure 4.12: Dust Attenuation for Measured Dust and Sand Particles Distribution

Table 4.4 presents the peak values of point and total dust and sand induced attenuations taken from Fig. 4.6 – Fig. 4.11 for different scenarios of particle's distributions and frequency range.

Table 4.4: Point and Dust Attenuation Peak Values Comparison

$Dust\ and\ Sand\ Distribution$	$Peak\ A_p$	$Peak\ A_D$
$Uniform$	1.5	4.5
$Normal$	1.7	5.2
$Experimental$	1.3	3.2

CHAPTER 5

ENHANCED DECISION SYSTEM

An EDS has to perceive its environment and to interact with other agents. The system in this research is used to improve SNR according to weather’s variation. These capabilities are derived through appropriate tuning of parameters such as power, modulation, coding, frequencies and data rates. They are integrated to achieve an immune communication behavior in accordance with the variations in weather conditions [61], [62]. Thus, the simulated EDS checks out various combinations for different input variables based on a given threshold signal level at each block and conveys intelligently the ultimate value for SNR.

The EDS is proposed in this thesis to improve end-to-end satellite communications under different weather conditions until best SNR values were achieved. The EDS starts by holding input signal parameters such as frame size, propagation angle and SNR estimated values that were compared against threshold level, in a single database. Then it illustrates a manner for changing parameters of the satellite system in order to overcome the atmospheric impairments such as dust and sand storms, and to increase reliability of the data transmitted throughout the channel. The simulation and results for SNR improvements by using EDS will be discussed in the later sections of this chapter. Fig. 5.1 presents the SNR estimations before incorporating the proposed EDS.

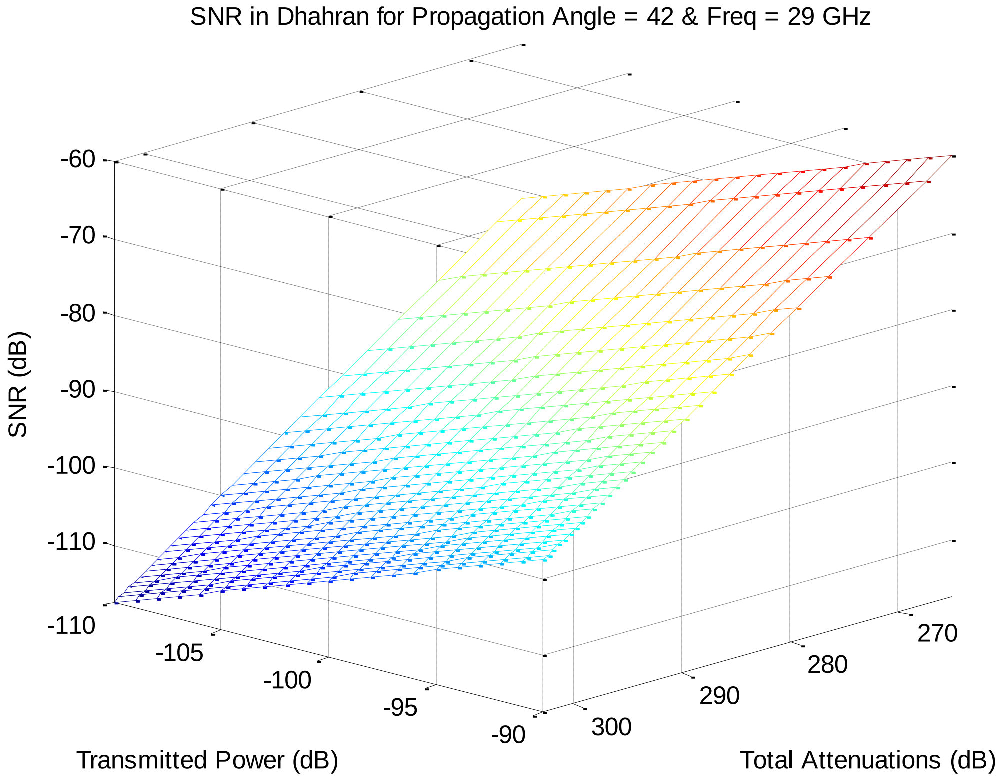

Figure 5.1: Satellite Link SNR before Enhanced System Adjustments

5.1 Signal to Noise Ratio Improvement

The proposed EDS plays its role in improving QoS by virtue of improving SNR and by maximizing system throughput and availability of the links. The estimation techniques of signal attenuation presented in previous sections are used by EDS to understand current link characteristics and in finding optimally desired adjustments in the link connection and the queuing characteristics in conjunction with DSS [1].

5.2 Schematics of Control

The proposed EDS proficiently searches for different combinations of input control variables such as transmit power level, modulation schemes, channel coding, and transmission rates to minimize estimated attenuation effect and maximize channel robustness and efficiency by improving SNR. The relationship of different control modules of EDS is shown in Fig. 5.2.

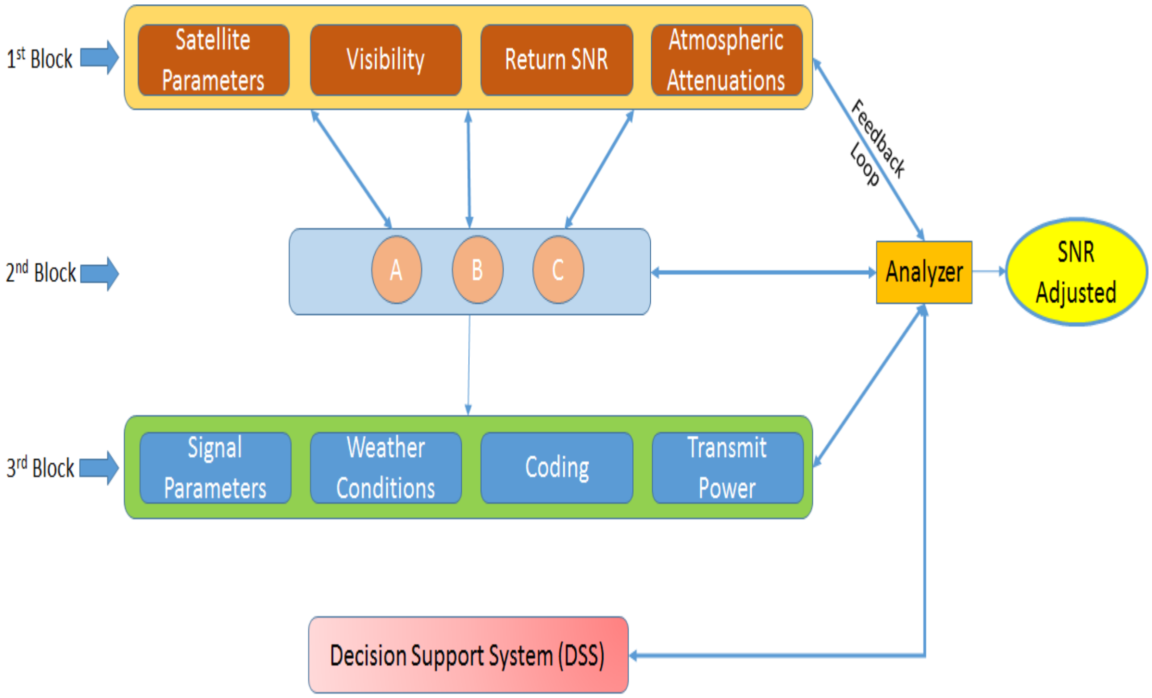

Figure 5.2: Enhanced Decision System (EDS)

The first control block collects signal parameters such as satellite parameters that are presented by data rate, propagation angle, frame size, frequency, and signal transmit power. Alongside, environmental factors such as measurements, computing constraints, antenna gains, dish diameters, atmospheric attenuation, and refresh durations, along with the SNR feedback, and measured visibility.

The second control block compares the differences between the estimated SNR for the impending weather conditions and the SNR threshold value set by the system's designers. This comparison leads to one of three different possible outcomes {A, B, and C} as shown in Fig. 5.2. In case of the first outcome {A}, where estimated SNR is smaller than the threshold, the controller will decide to increase transmitted power up to a maximum safety limit. In case of the second outcome {B}, where estimated SNR is equal to or greater than the threshold level, the DSS will be satisfied and will jump to the last block. In case of the third outcome {C}, where estimated SNR is smaller than the threshold level even after increasing the transmitted power to its maximum value, the controller will go to the next block for more diagnostics.

In the third control block, based on adjusted SNR value, the controller will search for the adjustment of other parameters such as data rate, modulation, and coding values. If the threshold level value can be reached by using any of the different variable combinations, then the controller will decide to move to the last block for the final decision.

The analyzer and DSS, in the control block, have to determine whether the combinations presented by the third control block achieve the desired SNR range. If the third control block failed to produce desired SNR range, it would then, through the feedback control loop, ask the first control block to make the necessary modifications as per specified refresh duration. The analyzer and DSS block will compare the different SNR values achieved by different combinations and select the suitable one based on the available conditions and requirements.

The feedback system will continue iterating according to DSS decision or until a satisfactory value is reached. If the problem persisted even after a given number of iterations, the DSS is designed to bring the system's capacity to a lower level and curtail services to customers as per rules sanctioned by the designers. Thus, the system will have the ability to modify data rate, frame size, modulation and coding. for SNR adjustments in special cases such as horrendous weather conditions.

5.3 Analyzer and DSS

The simulated model of EDS was developed so as to understand what level of signal improvement could be made given that we have a better way of predicting atmospheric attenuation as described earlier. The EDS consists of different control blocks that receives user commands and high level operational logic from analyzer whose internal block diagram is given in Fig. 5.2. The analyzer role with DSS is constructed from specific classes of computerized algorithms that support satellite signal decision-making activities. Typical functions that an analyzer might perform include:

- Accessing all of our current information assets, such as knowledge base, data prediction, and given satellite elements to identify and to improve received satellite signals under different weather conditions.
- Applying different combinations of satellite relevant parameters at each stage in an efficient manner to satisfy designers' threshold values as well as customer requirements.

- Controlling SNR values to an appropriate level during the simulation processes to fit within designers' recovery signal values.

The analyzer along with DSS acts to maintain QoS and service level agreements (SLAs) by adjusting satellites' signal propagation parameters during precarious weather conditions. It takes in the estimated weather data and proficiently searches for different combinations of controllable input variables such as transmit power level, modulation schemes and channel coding rates. to minimize the estimated attenuation effect and maximize the channel robustness and efficiency by improving SNR and subsequent QoS improvements as depicted in Fig. 5.2.

5.4 Algorithmic Basis for SNR Calculation

In satellite communications the most prominent contributors to noise beside rain and free space are dust and sand storms usually occurring in desertified regions [3], [63]. Thermal noise power spectral density can be calculated as: $N_o = K\,.T,$ where Boltzmann constant $K = 1.38\ \times 10^{-23}\ {}^{Ws}/_{K} = -228.6\ {}^{dBWs}/_{K}$ and effective noise temperature $T = T_a +\ T_r$, where T_a is noise temperature of the antenna, and T_r is noise temperature for the receiver represented as $T_r = \left(10^{{}^{N_r}/_{10}} - 1\right) \times 290\ K,$ with noise figure of low-noise amplifier, $N_r\ \approx 0.7 \sim 2\ dB$. Thus, the ratio between signal and noise power spectral density is [3]:

$$\frac{C}{N_o} = \frac{C}{K\,.T} = \frac{P_r}{K\,.T} = \frac{P_t\,.\ G_t}{A_t}\,.\frac{G_r}{K\,.T}\,. \tag{5.1}$$

The total impairments (A_t) can be can be computed as a combination of dust and sand attenuation (A_D) and free space losses (A_o):

$$A_t = A_D + A_o \tag{5.2}$$

$$A_o = \left({}^{4\pi d}/_{\lambda}\right)^2 \tag{5.3}$$

where d is the distance between transmitter and receiver and wavelength $\lambda = {}^{c}/_{f}$.

$$E_s = C\,.T_s = {}^{C}/_{R_s} \tag{5.4}$$

Where, E_s is symbol energy, transmission rate is R_s (symbols/sec) being inversely equivalent to the symbol duration T_s and energy to noise power density per symbol [3], [5]:

$$\frac{E_s}{N_o} = \frac{C}{N_o}\,.T_s = \frac{C}{N_o}\,.\,\frac{1}{R_s}, \tag{5.5}$$

or,

$$\frac{E_s}{N_o} = C - N_o - R_s \;\; dB, \tag{5.6}$$

$$SNR\,(A_t, P_t) \;=\; P_t + G_t - A_t + G_r - T - K - R_s \qquad dB. \tag{5.7}$$

Where P_t and P_r are transmitter and receiver power and G_t and G_r are antenna gain at transmitter and receiver sides respectively.

5.5 Simulation Results and Discussions

Fig. 5.1 gives us a clear view about the variation of SNR with different dust radius and wavelength. Moreover, the result can be used as key factors in implementing an enhanced engine that can act to improve end-to-end wireless communications. These results have been placed at KFUPM University campus station - Dhahran, Saudi Arabia. The satellite dish is 100 *m* above sea level.

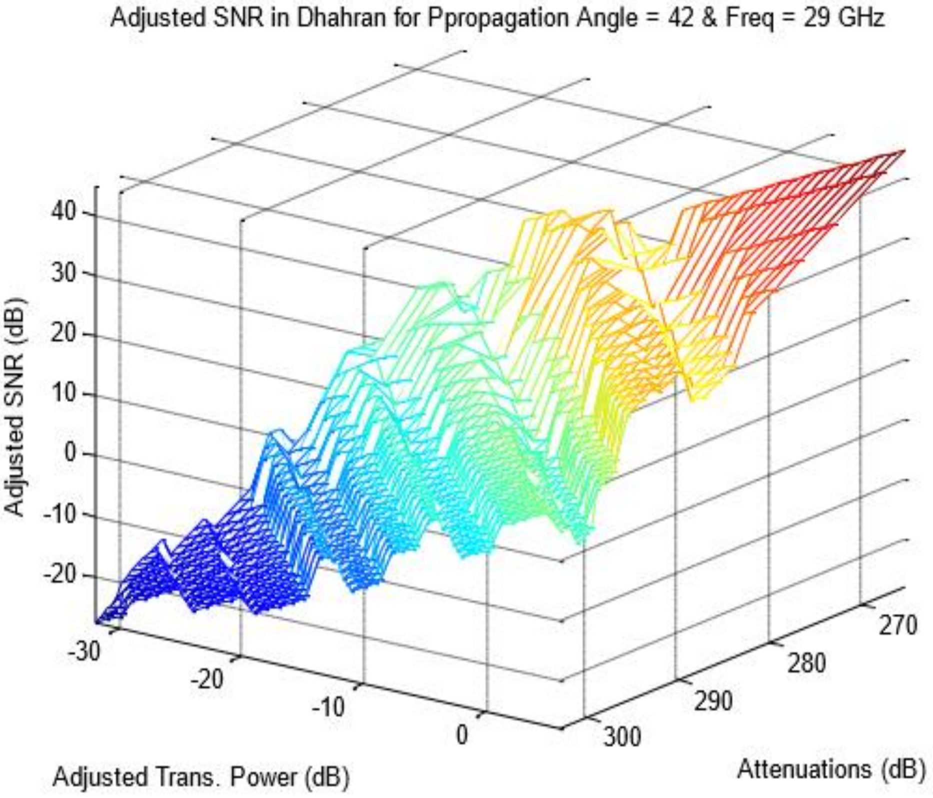

Figure 5.3: Satellite Link SNR after Enhanced System Adjustments

Fig. 5.1 and Fig. 5.3 compare the SNR values before and after the application of EDS control respectively while subjecting the channels to the same weather attenuation (with total attenuation ranging from $264 \sim 302\ dB$ at an operational frequency of $29\ GHz$ and propagation angle 42^o in both results. When EDS control is turned off, the SNR ranged between $(-90 \sim -60)\ dB$ and transmit power ranged between $(-110 \sim -90)\ dB.$ All conditions being the same, the activation of EDS control made it possible to markedly improve the SNR to $(-16 \sim 44)\ dB$ range by means of raising the transmit power between $(-30 \sim 6)\ dB$ range, along with adjustments made in modulation and coding.

CHAPTER 6

CONCLUSIONS AND FUTURE WORK

This chapter provides a summary of the research that is presented in this thesis. The basics of satellite communication have been described, covering the applications of satellite technology and the operational frequencies. Different weather anomalous conditions and their respective influences on the radio links of satellites and earth stations have been described briefly. A thorough literature survey related to the forecast mechanisms, characteristics of dust and sand storms and several factors influencing such weather conditions have been presented. Lastly, the signal improvements due to incorporation of an EDS have been highlighted.

A modified strategy based on horizontally layering the dust and sand storms is being devised in order to gain a close to real time attenuation estimation. Several experimental techniques such as the sieve and hydrometer test have been applied in order to gather the dust and sand particles distribution details in the region of Saudi Arabia. Based on the assumed and experimental dust and sand distributions, impairment computations including the point and dust attenuation have been done. Finally, an EDS has been designed to counter the weather impairments on radio channel due to dust and sand storms.

6.1 Conclusions

Dust and sand storms are usually regarded as a complex meteorological phenomenon being of uncorrelated nature for different regions. Similarly, the altitude based non-uniformity of visibility and several environmental factors during a dust and sand storm are difficult to be predicted or estimated with accuracy. Therefore, the environmental factors and mathematical parameters details related to the dust and sand storm events have been reviewed. Visibility is a key parameter which is upon which the accuracy of point and dust estimations depends a lot.

In this work, a modified approach has been devised in order to physically model the dust and sand storms by making horizontal layers on the basis of vertical visibility variations. Taking into account the regional uncorrelated nature of dust and sand samples and storms for different regions of world, the forecasted and real time measurements have been done. This data has been utilized in estimating the point and total dust and sand induced impairments.

Finally, an EDS is designed in order to improve the satellite link SNR during such weather deteriorated conditions. The EDS has three possible cases of working based on the SNR estimates at the input i.e. no adjustment required, only power increase and reconfiguration of several signal parameters.

6.2 Future Work

The recommendations for further research in this work are listed as follows:

- To devise an approach of making three dimensional layers for dust and sand storms, in order to get a better physical understanding of the phenomenon of such storms.
- In this research the forecast data related to dust and sand storms is presented only. A strategy could be devised to incorporate such weather forecasts to attain a priori impairment estimation.
- The presence of moisture induces a variation in the real and imaginary dielectric constants of dust and sand particles. Therefore, the cohesive impairment effects of moisture along with dust and sand particles can be investigated.
- The technique of SEM/EDX can be used in order to gather the geometric features, chemical composition and size distribution of dust and sand particles.
- Experimental values of the key parameter visibility may also be gathered during the dust and sand storms effected durations with the help of a visibility sensor.

REFERENCES

[1] O. Butt, K. Harb, and S. Abdul-Jauwad, “Intelligent Decision System for Measured Dust Distributions Impairing Satellite Communications,” in IEEE International Conference on Computational Intelligence and Virtual Environments for Measurement Systems and Applications, Ottawa, Ontario, Canada, May 2014.

[2] K. Harb, A. Srinivasan, C. Huang, and B. Cheng, “Qos In Weather Impacted Satellite Networks,” in IEEE Pacific Rim Conference on Communications, Computers and Signal Processing, pp. 178–181, 2007.

[3] K. Harb, O. Butt, S. Abdul-Jauwad, and A. M. Al-Yami, “Systems Adaptation for Satellite Signal Under Dust , Sand and Gaseous Attenuations,” J. Wirel. Netw. Commun., vol. 3, no. 3, pp. 39–49, 2013.

[4] K. Harb, O. Butt, A. A. Al-Yami, and S. Abdul-Jauwad, “Probabilistic Dust Storm Layers Impacting Satellite Communications,” in proc. of the IEEE International Conference on Space Science and Communication (ICONSPACE), pp. 407–411, July 2013.

[5] K. Harb, B. Omair, S. Abdul-Jauwad, A. Al-Yami, and Ab. Al-Yami, “A Proposed Method for Dust and Sand Storms Effect on Satellite Communication Networks,” in Innovations on Communication Theory (INCT), pp. 4–8, Oct. 2012.

[6] Elsheikh, M. R. Islam, K. Al-Khateeb, A. Z. Alam, and Z. O. Elshaikh, “A Proposed Vertical Path Adjustment Factor for Dust Storm Attenuation Prediction,” in 4th International Conference on Mechatronics (ICOM), pp. 1–3, May 2011.

[7] "European Space Agency (ESA), Satellite Frequency Bands" website: http://www.esa.int, last accessed date Jan 2014.

[8] "Istituto Nazionale Di Geofisica E Vulcanologia (INGV), Ionospheric Scintillation" website: http://roma2.rm.ingv.it, last accessed date Jan 2014.

[9] "University of Portsmouth, Department of Electronic and Computer Engineering, Research Cluster Website, Research areas – Satellite and Terrestrial Telecommunications – Dynamic Microscale Rain Structure" website: http://research.ee.port.ac.uk, last accessed date Jan 2014.

[10] "Weather and Sea State Forecast, Environmental Protection Department, Saudi Aramco" website: http://www.wassf.net/, last accessed date Jan 2014.

[11] "University of Illinois At Chicago (UIC), Civil Engineering, Mechanics and Metallurgy, Soil Mechanics Laboratory, Grain Size Analysis" website: http://www.uic.edu/uic/, last accessed date Dec. 2013.

[12] Jervase, Joseph A., and Sami M. Sharif. "Influence of dust storms and reflector tolerance on cross polarization of earth satellite links." In Proc. Arabsat Symp., Riyadh, Saudi, pp. 166-169. 1988.

[13] "ITU Recommendation ITU-R Rpn.618-4," 2003.

[14] "Reports of the CCIR: Report 563-4, CCIR XVII th Plenary Assembly, Dusseldorf," May 1990.

[15] A. Paraboni, "Testing of Rain Attenuation Prediction Methods Against the Measured Data contained in the ITU-R Data-bank," ITU-R Study Group 3 Document, sr 2-95/6, Switzerland, 1995.

[16] E. Salonen, "Prediction Models of Atmospheric Gases and Clouds for Slant Path Attenuation," in proc. of the Olympus Utilization Conference, 1993.

[17] D. Slobin, "Microwave Noise Temperature and Attenuation of Clouds : United States, Alaska and Hawaii," vol. 17, no. 6, pp. 1443–1454, 1982.

[18] M. Altshuler, Edward E., "Cloud Attenuation at Millimeter Wavelengths," Antennas Propagation, IEEE Trans., vol. 37, no. 11, pp. 1473–1479, 1989.

[19] C. Gerace and E. K. Smith, "A Comparison of Cloud Models," IEEE Antennas and Propagation Magazine, pp. 32–38, Oct. 1990.

[20] J. Batten, "Radar Observations of the Atmosphere," 1973.

[21] M. Dissanayake, A. W., "Radar and Attenuation Properties of Rain and Bright Band," Antennas Propag., vol. 1, pp. 125–129, 1978.

[22] Z. Kharadly and A. S. V. Choi, "A Simplified Approach to the Evaluation of EMW Propagation Characteristics in Rain and Melting Snow," IEEE Trans. Antennas Propag., vol. 36, no. 2, pp. 282–296, 1988.

[23] S. Wang, S. G., G. R. Dong, D. B. Yang, and J. Jin, “A Study on Sand-Dust Storms over the Desert Region in North China,” J. Nat. Disasters, vol. 5, no. 2, pp. 86–94, 1996.

[24] D. Joseph, and D. K. Raipal, “‘Andhi’ The Convective Dust Storms of Northwest India, Mausam 31,” pp. 431–442, 1980.

[25] J. Brazel and W. G. Nickling, “The Relationship of Weather Types to Dust Storm Generation in Arizona (1965-1980),” J. Climatol., vol. 6, no. 3, pp. 255–275, Jan. 1986.

[26] E. Jauregui, “The Dust Storms of Mexico City,” Int. J. Climatol., vol. 9, no. 2, pp. 169–180, March 1989.

[27] Ott, S. T., A. Ott, D. W. Martin, and J. A. Young, “Analysis of a Trans-Atlantic Saharan Dust Outbreak Based on Satellite and Gate Data,” Mon. Weather Rev., vol. 119, no. 8, pp. 1832–1850, 1991.

[28] Hankin F. H., “On the Dust-Raising Winds and Descending Currents," India Met. Memoirs, vol. XXII, Part VI, 567, 1921.

[29] J. Sutton, “Haboobs,” Q. J. R. Meteorol. Soc., vol. 51, no. 213, pp. 25–30, 1925.

[30] X. Wang, Z. Dong, J. Zhang, and L. Liu, “Modern Dust Storms in China: An Overview,” J. Arid. Environ., vol. 58, no. 4, pp. 559–574, Sept. 2004.

[31] C. Sun, Leng, Xukai Zhou, Juntian Lu, and Yong-Pyo Kim, “Climatology, Trend Analysis and Prediction of Sandstorms and their Associated Dustfall in China,” Water, Air Soil Pollution, vol. 3, no. 2, pp. 41–50, 2003.

[32] J. Novlan, M. Hardiman, and T. E. Gill, “A Synoptic Climatology of Blowing Dust Events in El Paso , Texas from 1932-2005,” Am. Meteorol. Soc. J., vol. 3, 2007.

[33] “Comet (Cooperative Program for Operational Meteorology), Mesoscale Primer. Forecasting Dust Storms. University Corporation for Atmospheric Research.” 2003.

[34] D. Model, J. Goldhirsh, and L. Fellow, “Attenuation and Backscatter from a Derived Two-Dimensional Duststorm Model,” IEEE Trans. Antennas Propag., vol. 49, no. 12, pp. 1703–1711, 2001.

[35] Bashir, S. O., and N. J. McEwan. "Microwave Propagation in Dust Storms: A Review," IEEE Proc. H (Microwaves, Antennas Propagation), vol. 133, no. 3, pp. 241–247, 1986.

[36] J. Goldhirsh, "A Parameter Review and Assessment of Attenuation and Backscatter Properties Associated with Dust Storms Over Desert Regions in the Frequency Range of 1 to 10 GHz.," Antennas Propagation, IEEE Trans. 30.6, pp. 1121–1127, 1982.

[37] Ghobrial, Samir I., and Joseph A. Jervase., "Microwave Propagation in Dust Storms at 10.5 Ghz - A Case Study in Khartoum, Sudan," IEICE Trans. Commun., vol. E80-B, pp. 1722–1727, 1997.

[38] Ghobrial, SAMIR I., and S. A. M. I. M. Sharief., "Microwave Attenuation and Cross Polarization in Dust Storms," IEEE Trans. Antennas Propag., vol. 35, no. 4, pp. 418–425, April 1987.

[39] Elsheikh, M. R. Islam, A. H. M. Z. Alam, A. F. Ismail, K. Al-Khateeb, and Z. Elabdin, "The Effect of Particle Size Distributions on Dust Storm Attenuation Prediction for Microwave Propagation," International Conference on Computer and Communication Engineering, pp. 1–5, May 2010.

[40] Z. Elabdin, M. R. Islam, O. O. Khalifa, and H. E. A. Raouf, "Mathematical Model for the Prediction of Microwave Signal Attenuation due to Duststorm," vol. 6, pp. 139–153, 2009.

[41] Z. Elabdin, M. R. Islam, O. O. Khalifa, and A. F. Ismail, "Duststorm Measurements for the Prediction of Attenuation on Microwave Signals in Sudan," in International Conference on Computer and Communication Engineering, pp. 1181–1185, 2008.

[42] Q. Dong, Y. Li, J. Xu, H. Zhang, and M. Wang, "Effect of Sand and Dust Storms on Microwave Propagation," IEEE Trans. Antennas Propag., vol. 61, no. 2, pp. 910–916, 2013.

[43] Ahmed, Abobakr S., Adel A. Ali, and Mohammed A. Alhaider., "Dust Size Analysis for Tropospheric Propagation of Millimetric Waves into Dust Storms," IEEE Trans. Geosci. Remote Sens., no. 5, pp. 593–599, 1987.

[44] H. Chen, S. Member, and C. Ku, “Calculation of Wave Attenuation in Sand and Dust Storms by the FDTD and Turning Bands Methods at 10 – 100 GHz,” IEEE Trans. Antennas Propag., vol. 60, no. 6, pp. 2951–2960, 2012.

[45] Abuhdima, Esmaeil Mohamed, and Ibrahim Mohamed Saleh., “Effect of Sand and Dust Storms on Microwave Propagation Signals in Southern Libya,” in Melecon 2010 15th IEEE Mediterranean Electrotechnical Conference, pp. 695–698, 2010.

[46] S. Estabrook, Polly, John Huang, and William Rafferty, “A 20/30 GHz Personal Access Satellite System Design,” in IEEE International Conference on Communications (ICC), (Boston, Ma), pp. 216–222, 1989.

[47] F. Davarian, “Earth-Satellite Propagation Research,” IEEE Communications Magazine, pp. 74–79, April 1994.

[48] T. Lows, S. Member, and T. A. Russell, “Propagation Considerations for Emerging Satellite Communications Applications,” vol. 81, no. 6, 1993.

[49] Lu, Q. Zhang, and Z. Zhao, “SVM in the Sand-Dust Storm Forecasting,” in IEEE International Conference on Machine Learning and Cybernetics, pp. 13–16, Aug. 2006.

[50] M. Abuhdima, and I. M. Saleh, “Effect of Sand and Dust Storms on GSM Coverage Signal in Southern Libya,” in International Conference on Electronic Devices, Systems and Applications, pp. 264–268, 2010.

[51] M. Patterson, “Atmospheric Extinction Between 0.55 mm and 10.6 mm due to Soil-Derived Aerosols,” Appl. Opt., vol. 16, pp. 2414–2418, 1977.

[52] M. Levin, Zev, and Joachim H. Joseph, “Properties of Sharav (Khamsin) Dust-Comparison of Optical and Direct Sampling Data,” J. Atmos. Sci., vol. 37, no. 4, pp. 882–891, 1980.

[53] J. Schütz, Lothar, “Particle Number and Mass Distributions above 10^{-4} cm radius in Sand and Aerosol of the Sahara Desert,” J. Appl. Meteorol., vol. 13, no. 8, pp. 863–870, 1974.

[54] Gillette, I. H. Blifford, and D. W. Fryrear, “The Influence of Wind Velocity on the Size Distributions of Aerosols Generated by the Wind Erosion of Soils,” J. Geophys. Res., vol. 79, no. 27, pp. 4068–4075, Sep. 1974.

[55] R. King, Michael D., Dale M. Byrne, and Benjamin M. Herman, “Aerosol Size Distributions obtained by Inversions of Spectral Optical Depth Measurements,” J. Atmos. Sci. 35, vol. 35, no. 11, pp. 2153–2167, 1978.

[56] S. Ahmed, “Role Of Particle-Size Distributions on Millimetre-Wave Propagation in Sand/Dust Storms,” IEEE Proc. H (Microwaves, Antennas Propagation), vol. 134, no. 1, pp. P. 55–59, 1987.

[57] K. Harb, F. R. Yu, P. Dhakal, and A. Srinivasan, “Performance Improvement In Satellite Networks Based on Markovian Weather Prediction,” in IEEE Global Telecommunications Conference Globecom, pp. 1–5, 2010.

[58] A. Ahmed, Abobakr S., and Adel A. Ali, "Measurement of Atmospheric Particle Size Distribution During Sand/Duststorm in Riyadh, Saudi Arabia," Atmos. Environ., vol. 21, no. 12, pp. 2723–2725, 1987.

[59] V. Hippel, "Dielectric Materials and Applications," Cambridge, Ma: Mit Press, 1954.

[60] K. Njoku, and Eni G., "Theory for Passive Microwave Remote Sensing of Near Surface Soil Moisture," J. Geophys. Res., vol. 82, no. 20, pp. 3108–3118, 1977.

[61] "Telesat Canada, ISS (Intelligent Satellite Service) Research and Development" website: http://www.telesat.ca, last accessed date March 2014.

[62] M. Bousquet, Satellite Communications Systems. John Wiley & Sons Ltd, UK. 1993.

[63] E. Lutz, and M. Werner, "Satellite Systems for Personal and Broadband Communications. Springer", New York. 2000.

VITAE

Name: Muhammad Omair Butt

Nationality: Pakistan

Date of Birth: 11/13/1988

Email: omairbutt@outlook.com

Address: KFUPM Student Housing, Dhahran, Saudi Arabia

Academic Background: MS Electrical Engineering, KFUPM (2014)

: Bachelor in Telecom Engineering, FAST-NU (2010)

Publications:

- **B. Omair**, Kamal Harb, and Samir H. Abdul-Jauwad, "Intelligent Decision System for Measured Dust Distributions Impairing Satellite Communications", IEEE International Conference on Computational Intelligence and Virtual Environments for Measurement Systems and Applications (CIVEMSA), Ottawa, Ontario, Canada, 5-7 May 2014.

- Kamal Harb, **B. Omair**, Samir H. Abdul-Jauwad, and Abdulaziz Al-Yami, "Systems Adaptation for Satellite Signal under Dust, Sand and Gaseous Attenuations", Journal of Wireless Networking and Communications, Vol. 3, No. 3, pp. 39-49, 2013.

- Kamal Harb, **B. Omair**, Abdulaziz Al-Yami, and Samir H. Abdul-Jauwad, "Probabilistic Dust Storm Layers Impacting Satellite Communications", Proc. of the IEEE International Conference on Space Science and Communication (IconSpace), Malacca, Malaysia, pp. 407-411, July 2013.

- Kamal Harb, **B. Omair**, Samir H. Abdul-Jauwad, A. Al-Yami, and Ab. Al-Yami, "A Proposed Method for Dust and Sand Storms Effect on Satellite Communication Networks", Innovations on Communication Theory (INCT), Istanbul, Turkey, pp. 33-37, Oct. 2012.